



Micro/nanoscale magnetic robots for biomedical applications

M. Koleoso^{a,1}, X. Feng^{a,1}, Y. Xue^a, Q. Li^b, T. Munshi^c, X. Chen^{a,*}

^a School of Engineering, Institute for Bioengineering, The University of Edinburgh, King's Buildings, Mayfield Road, Edinburgh EH9 3JL, UK

^b School of Engineering, Institute for Energy Systems, The University of Edinburgh, King's Buildings, Mayfield Road, Edinburgh EH9 3JL, UK

^c School of Chemistry, University of Lincoln, Brayford Pool, Lincoln, Lincolnshire, LN6 7TS, UK



ARTICLE INFO

Keywords:

Micro/nanorobots
Magnetic actuation
Biomedical applications
Cargo delivery
Clinical availability

ABSTRACT

Magnetic small-scale robots are devices of great potential for the biomedical field because of the several benefits of this method of actuation. Recent work on the development of these devices has seen tremendous innovation and refinement toward improved performance for potential clinical applications. This review briefly details recent advancements in small-scale robots used for biomedical applications, covering their design, fabrication, applications, and demonstration of ability, and identifies the gap in studies and the difficulties that have persisted in the optimization of the use of these devices. In addition, alternative biomedical applications are also suggested for some of the technologies that show potential for other functions. This study concludes that although the field of small-scale robot research is highly innovative there is need for more concerted efforts to improve functionality and reliability of these devices particularly in clinical applications. Finally, further suggestions are made toward the achievement of commercialization for these devices.

1. Introduction

Microrobots and nanorobots are small-scale manipulatable devices at the micrometer and nanometer scale which have found uses in several fields and have been noted to be of great interest in the biomedical field. The small size of these devices is of particular benefit in healthcare as it allows for much less invasive procedures to be used in place of surgery and non-targeted chemical and radiation therapies [1]. This greatly eases diagnosis and detection of diseases and reduces risk of infection, complications, side effects, and recovery time in patients [2–4]. They are also widely used for other laboratory-based biomedical applications such as genetic and tissue engineering, imaging, and investigations of biological fluid properties [5–7]. Their size, however, also puts limitations on options for powering and manipulation, with onboard energy storage and/or conversion posing several obstacles in conceptualization. Several reviews have been published, broadly explaining a range of methods to manipulate and actuate milli/micro/nanorobots, including the use of chemically powered motors, acoustic propulsion, and ultrasound energy [4,8,9], and their applications in drug delivery, precision surgery, sensing, and detoxification [10–12]. Some of these reviews cover very broad topics including milli/micro/nanorobots with different actuation mechanisms with a brief review of each category and comparison,

whereas some others focus on strategies of actuation [13]. The main focus of this review, however, will be on microscale and nanoscale robots actuated using magnetic fields and the systematic summary and discussion of their actuation approaches and applications in biomedical field. The use of magnetic fields for manipulation is of advantage in biomedicine because of their minimal interaction with tissues below magnetic field magnitudes of 3 Tesla (T) and the body's transparency to them [14].

Early applications of magnetic nanotechnology in biomedicine mainly consisted of the use of magnetic nanoparticles (MNPs) whose manipulation greatly relied on how magnetic materials respond to magnetic field gradients [15,16]. These applications include cell labeling, magnetic separation for lab analysis and synthesis, imaging, magnetic drug targeting, hyperthermia, and diagnosis among others [17–20]. However, biomedical small-scale robots normally need to perform their tasks in fluidic environments with low Reynolds numbers. Because of their relatively small size, they tend to face high drag forces and inertia vacancy when operating in these environments. The use of magnetic gradients for propulsion in such environments may present low precision control and jerky movements [21]. In view of this, more efficient actuating methodologies and propulsion efficacy than those typically observed when using magnetic field gradients for manipulation are required.

* Corresponding author.

E-mail addresses: Michael.Chen@ed.ac.uk, xianfeng.chen@oxon.org (X. Chen).

¹ These authors contributed equally.

More recent developments involve the use of magnetic torque, rotating and oscillating magnetic fields, and other means to actuate nanorobots resulting in their propulsion and allowing for more accurate 2D and 3D navigation of these devices [22]. A lot of the propulsion methods of these devices have been adapted from nature, for example helical flagella found in some bacteria, tail-like flagella found in sperms, and other designs that mimic motion of fish in water [23–26]. There have also been more imaginative designs such as surface walkers and two-armed swimmers [27,28].

The field of biomedical magnetic micro/nanorobots is relatively new and still in its highly innovative stage. As illustrated in Fig. 1, the number of papers published in this field over the past five years (2015–2019) is greater than the total number of publications in the field over the twenty-five years prior. This paper aims to investigate the current state of the art of biomedical magnetic nanorobots and microrobots, their propulsion mechanisms, fabrication methods, current applications, and the technologies they use. The further incorporation of other technologies or materials in designs for the purpose of improving biomedical functionalities and safety will also be systematically reviewed. There will be a brief comparison between microrobots and nanorobots, identifying where they outperform each other in biomedicine. Finally, the challenges faced in the use and implementation of these advancements *in vivo* will be looked at to identify areas for further research.

2. Recent advancements of the design of magnetic small-scale robots

2.1. Introduction to magnetically actuated micro/nanorobots

2.1.1. General fabrication methods

To manufacture a magnetically actuated micro/nanorobot, a magnetic component should be involved in the structure of micro/nanorobots. Thus, as summarized in Fig. 2, the general and most widely adopted fabrication technologies for magnetic small-scale robots often contain two sections: micro/nanorobots fabrication and incorporation of the magnetic component.

The first step is establishing the basic structure of robots which can be achieved through several routine nanolithography techniques that etch (write on) or polymerize photosensitive materials. Etching methods typically make use of UV light (photolithography), laser (two-photon

lithography/direct laser writing/3D laser lithography), electron beams (E-beam lithography), and X-ray (X-ray lithography) [29–32]. Other strategies used in establishing 3D structure include glancing angle deposition (GLAD) which is based on physical vapor deposition, template-assisted electrodeposition, and use of a more advanced bio-template technique [23,33–35]. Besides, the bodies of the magnetic robots can also be made of soft materials with the use of soft smart materials recently seeing a rise [36,37]. This is due to their improved functionality and better mimicry of organisms that inspire their designs than their rigid counterparts.

To allow for magnetic manipulation, the second step requires the incorporation of magnetic components into the micro/nanorobots which could be the partial or complete magnetic material coating of the robot body, the connection of magnetic segments, and the use of magnetic micro/nanoparticles (detailed methods in Fig. 2). However, more and more recently developed novel fabrication methods are in efforts to simplify the manufacturing process or to fabricate robots with special structures. These methods will be discussed in more detail mainly in Section 3.3.

2.1.2. Magnetic actuation mechanisms

The magnetic force (F) on a magnetic object with the magnetic dipole moment (m) due to a magnetic field (B) is equal to $(m \cdot \nabla)B$. When the magnetic field is homogeneous (gradient, ∇ , is zero), the magnetic robot will not experience gradient force and move along with the field but the magnetic torque, $\tau = m \cdot B$, can force the magnetic robot to align its dipole moment with the applied magnetic field via rotation if they are not in the same direction [41]. Thus, as illustrated in Fig. 3, magnetic fields utilized for robots propulsion must be time-varying (for example, rotating, oscillating, and stepping magnetic fields) or inhomogeneous (field gradients). These fields are normally generated from permanent magnet systems, electromagnet coil systems, or magnetic resonance imaging (MRI) machines. The different mechanisms of magnetic actuation will be described in detail next.

2.1.2.1. Interactions of time-varying magnetic fields with micro/nanorobots. Time-varying magnetic fields actuate magnetic devices through magnetic torque and often propel magnetic devices by inducing various types of motion. Time-varying magnetic fields can be classified as rotating, oscillating, and stepping magnetic fields. Rotating magnetic fields are one of the most commonly used time-varying fields. They are often used to actuate helical robots, one of the most widely used designs of microrobots or nanorobots whose actuation is achieved by the induction of rolling, corkscrew, and spin-top motions [42–44]. It has been found in the literature that the magnetic particle aggregates and some other interesting structures can be manipulated by rotating magnetic fields as well [45–50].

Oscillating magnetic fields normally center on flexible robots whose developments will be the focus of section 2.2.1. Stepping magnetic fields are a type of periodic magnetic field with ON/OFF phases. They can induce the wave-like motion of the magnetic cilium on a robot resulting in a power stroke to induce movement [51].

2.1.2.2. Interactions of magnetic field gradients with micro/nanorobots. Older magnetic micro/nanorobot designs typically made use of magnetic field gradients to manipulate magnetic micro/nanoparticles. As touched upon earlier, the use of magnetic gradients for the propulsion of micro/nanorobots presents some issues, especially if these devices are to be used *in vivo*. The magnetic force due to the magnetic gradient experienced by a magnetic material varies directly with the volume of magnetic material present. This relationship poses a hurdle to the maintenance of the nanoscale size for some applications if magnetic gradients are to be used as the means of propulsion.

To acquire more precise control using field gradients, 3D field gradients have been introduced. For example, Schuerle et al. [52] used eight

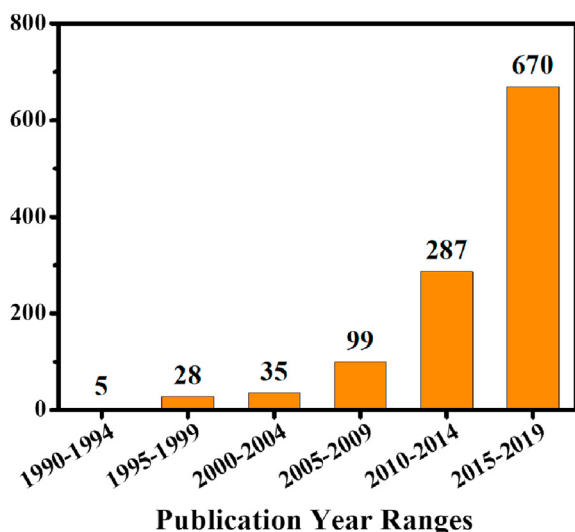


Fig. 1. The publication trends in magnetic small-scale robots showing the cumulative number of publications from 1990 to 2019 (including 2019) and the numbers of publications over five-year periods within this time range from the Web of Science. The key words used in the search were magnetic AND micro(nano)robots/machines/swimmers/propellers/motors.

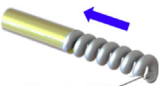
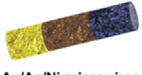

Micro/nanorobots fabrication	Magnetic component	
<ul style="list-style-type: none"> • Photolithography • Two-photon lithography/ Direct laser writing / 3D laser lithography • Glancing angle deposition • Template-assisted electrodeposition • Biotemplate method 	 <p>Ni coated Pd helical structure</p>	<ul style="list-style-type: none"> ▪ Magnetic films <ul style="list-style-type: none"> • e-beam evaporation • Physical vapor deposition/ sputter deposition • Dip-coating
	 <p>Au/Ag/Ni microwires</p>	<ul style="list-style-type: none"> ▪ Magnetic segments <ul style="list-style-type: none"> • Electrodeposition • Oblique angle deposition
	 <p>Hydrogel Microrobot</p>	<ul style="list-style-type: none"> ▪ Magnetic particles <ul style="list-style-type: none"> • Dip-coating • Emulsion method

Fig. 2. General fabrication methods for magnetic micro/nanorobots contain two sections: micro/nanorobots fabrication and incorporation of magnetic components [38–40]. (All images are used with permission).

stationary and independently controlled electromagnets to achieve the manipulation of magnetic micro/nanorobots moving in 3D space and proposed to use them in the single-cell manipulation and drug delivery. This manipulation system can generate field gradients up to 50 mT (5 T/m) and allow high degree-of-freedom (5) motion control. Beyond gradient-based pulling motion, the system can also manipulate the rocking motion and cork screw-like motion of microrobots when in combination with the rotating and stepping modes.

The existing MRI machines are promising tools for magnetic gradient pulling. The magnetic field gradients produced by MRI machines have been used to actuate devices with simple movement mechanisms resulting in what is termed as magnetic resonance navigation [53]. This could be of great use as if this method of actuation can be combined with MRI, it could provide a robust system for navigating devices through the human body while in the bore of MRI machines. A major challenge faced in the achievement of this sort of navigation, however, is the difficulty of simultaneously imaging and propelling devices as different pulse sequences are required for both of those functions meaning that one function is usually favored over the other. Recently, Felfoul et al. [53] attempted to show that this challenge can be overcome by working out an optimal pulse sequence that allows for propulsion at a suitable velocity

and imaging at a suitable frequency. Using this pulse sequence, a 2-mm chrome ball was steered through a complex vascular network phantom with velocities up to 74 mm/s while imaging at 27 Hz with a maximum gradient amplitude of 21 mT. Although this study was not conducted at the microscale or nanoscale, it acts as a proof of concept that magnetic gradient magnitudes previously thought only capable of propulsion can carry out simultaneous imaging and propulsion and show great potential for real-time image-guided navigation. By combining dynamic dipole field navigation (DFN-D) into clinical MRI, Shi et al. [54] produced a piezoelectric actuation system which can manipulate microcarriers moving in the vascular network. DFN-D can generate high field gradients in MRI by distorting the uniform magnetic field in an MRI scanner using precisely controlled ferromagnetic balls. The *in vitro* result showed that magnetic microparticles can accurately follow the planned trajectory and go into the targeted branch at the bifurcation point under the navigation of this system.

For more details of magnetic actuation mechanism, design, and operation, the readers are referred to several recently published reviews which have specifically introduced how magnetic fields (rotating, oscillating, and gradient) to actuate and control magnetic micro/nanorobots [55,56]. For example, in a very recent review, Yang and Zhang [57]

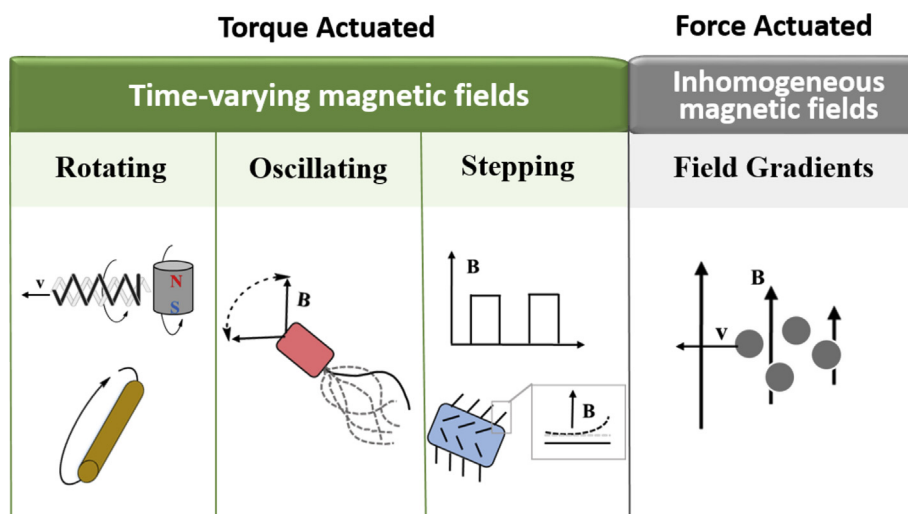


Fig. 3. Different magnetic fields for the actuation of different designs of magnetic micro/nanorobots.

elaborated actuation systems including systems with permanent magnets (single and multiple magnets) and systems with electromagnets (paired coils and distributed stationary or movable electromagnets). Beyond research examples, another recent review paper detailed current commercial magnetic actuation systems, such as Niobe, Genesis, Aeon Phocus, MiniMag, OctoMag, and Catheter Guidance Control and Imaging systems [58]. Fig. 4 displays typical electromagnetic actuation (EMA) systems from studies discussed by our review.

This section describes the fabrication of magnetic micro/nanorobots and the actuation mechanisms. Next, we will systematically describe the recent advancement in micro/nanorobot propulsion, micro/nanorobots design involving biological components such as bacteria, sperm, and integration of multiple functions in micro/nanorobots, as well as the biomedical applications of these wide ranges of micro/nanorobot systems.

2.2. Advancements in micro/nanorobot propulsion

2.2.1. Flexible swimmers

Flexible swimmers are those that have flexible parts, usually joints or tails allowing for deformations under the influence of a magnetic field. These devices are propelled because of an undulatory motion and are usually actuated by oscillating or rotating magnetic fields. There has been a recent rise in the study of these swimmers due to their improved swimming efficiencies and speeds when compared with the already extensively studied helical swimmers [23,61–64].

Jang et al. [65] investigated the locomotion of a magnetic three-link nanoswimmer that produced undulatory motion under an oscillating magnetic field resulting from the superimposition of two sinusoidal magnetic fields on x and y axes (Fig. 5a). This design is adapted from findings in the work by Purcell [66] where a three-link two-hinge swimmer produced the most efficient propulsion strategies at low Reynolds numbers. This was the first to investigate external actuation of Purcell's three-link swimmer. The design of this device consists of Nickel (Ni) links with flexible poly(allylamine hydrochloride) and poly(styrenesulfonate) polymer hinges. The swimmers are made using a version of the fabrication technique from Mirkovic et al. [67]. The technique was modified by using polypyrrole to make the flexible tail and the use of a deposition technique to produce the hinges which assured

consistency in them. The three-link swimmer produced an average speed of $14.44 \mu\text{m/s}$ or 0.93 body lengths per second. The findings of this paper suggest that the challenge of the use of magnetic nanorobots in highly viscous or low Re fluid environments, which are common in living organisms can be overcome. However, this work did not attempt to investigate another challenge which is the use of such nanorobots within living organisms, particularly areas very far from the skin surface [65].

Using a similar method of propulsion to the three-link nanoswimmer and inspired by the body and caudal fin (BCF) motion of fish in water, Li et al. [26] adapted the link and hinge design to produce a nanoswimmer (Fig. 5b) called the nanofish. BCF motion is a result of wave propagation along the bodies and tails of fish with their heads remaining relatively inactive. Thus, the propulsion of this swimmer differs from that of the three-link swimmer, in that, its body is magnetically actuated while the head and tail remain passive [68]. The fish-like nanoswimmer consists of a gold head, two nickel body segments, and a gold tail all linked by flexible, nanoporous silver hinges [26]. The swimmer produced its greatest speed of $30.9 \mu\text{m/s}$ at 11 Hz with speed decreasing at higher frequencies and showed immediate changes in speed in response to frequency adjustments. The nanofish's on-demand start-stop abilities were demonstrated by switching the actuating magnetic field off and on resulting in corresponding starting and stopping of its motion. It also demonstrated the ability to go through on/off cycles with minimal speed changes. To assess the effect of the lengths of components of this design, nanofish of different BCF-to-head length ratios were compared with those of larger BCF-to-head ratios achieving higher speeds. The researchers compared the speeds attained by the nanofish to those attained by other magnetically actuated swimmers at the time of publication and found that it achieved the greatest dimensionless speed (≈ 0.6 body length per revolution) [26].

Using the same fabrication technique, Li et al. [27] also produced a nanoswimmer inspired by human freestyle swimming motions as opposed to motions found in other organisms as is typically seen. This design researched a potentially more efficient propulsion method than others previously investigated, which possibly results from the kinematic optimization. This study demonstrates for the first time that an oscillating magnetic field can produce propulsion through motions other than planar oscillation or undulation. This swimmer portrayed in Fig. 5c is made up of a gold body and two magnetic nickel arms linked by flexible

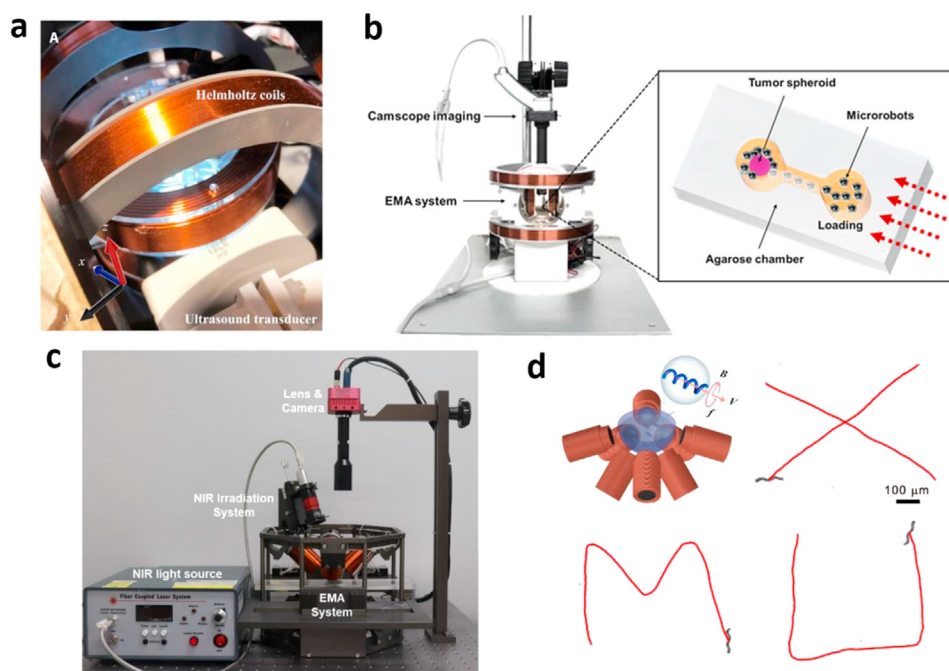


Fig. 4. Electromagnetic actuation (EMA) systems. (a) A triaxial Helmholtz coil electromagnetic system. Photo credit: Magdanz et al. [25]. (b) The comprehensive system for external active actuation and imaging of macrophage-based microrobots. “The EMA system consisted of three pairs of Helmholtz coils—one pair each on the x-axis, y-axis, and z-axis—and two pairs of Maxwell coils—one pair each on the x-axis and y-axis. The role of the three pairs of Helmholtz coils was to create a uniform magnetic flux, while the purpose of the two pairs of Maxwell coils was to induce a uniform gradient of magnetic flux in the region of interest” [59]. (c) The integrated eight-coil EMA and NIR system. In EMA system, four coils in the upper side and four coils in the down side [39]. (d) A commercial EMA system (MFG-100-I, MagnebotiX, Switzerland). Controlled locomotion along the trajectories of capital letters “XMU” (Xiamen University) [60]. (All images used with permission). NIR, near-infrared.

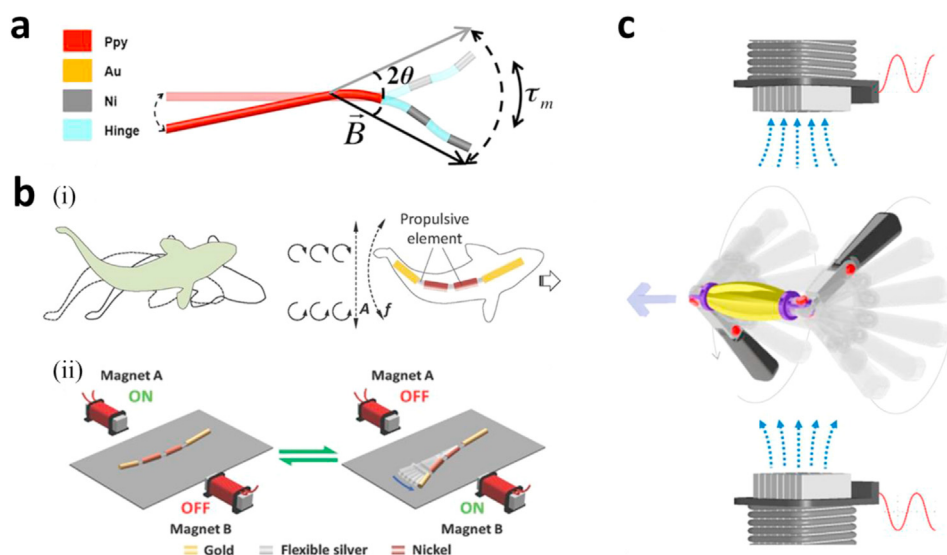


Fig. 5. Hard flexible magnetic micro/nanorobots and their magnetic actuation systems. (a) The schematic of the three-link nanoswimmer with undulatory motion, subjected to a magnetic field oscillation (2θ = angular sweep of the magnetic field, $B \rightarrow$ = magnetic field and τ_m = magnetic torque). A three-linked swimmer Ni ($\approx 1.75 \mu\text{m}$)–PAH/PSS ($\approx 1.5 \mu\text{m}$)–Ni ($\approx 1.75 \mu\text{m}$)–PAH/PSS ($\approx 1.5 \mu\text{m}$)–PPy ($\approx 9 \mu\text{m}$) [65]. (b) Artificial nanofish. (i) The Schematic of a natural fish and an artificial nanofish in BCF mode propulsion, involving passing undulatory waves down the entire length of the body. (ii) Magnetic propulsion of an artificial nanofish using a planar oscillating magnetic field [26]. (c) The schematic of two-arm nanoswimmers. Applying an oscillating magnetic field on z-direction leads to freestyle swimming of the nanorobot with two nanoarms wobbling alternatively to generate actuation in the x–y plane [27]. (All images are used with permission). BCF, body and caudal fin; PAH, poly(allylamine hydrochloride); PSS, poly(styrenesulfonate).

silver hinges. The components of the swimmer are made by template electrodeposition into a 200 nm alumina membrane template. The fabrication method allows for the creation of components of different lengths which has an effect on the flexibility of the silver hinges. An oscillating magnetic field resulting from two electromagnetic coils was used in the study. When compared with the three-link swimmer by Jang et al. [65] in which an undulatory movement was responsible for propulsion, the freestyle nanoswimmer shows much greater speeds (maximum speed of up to 12 body lengths per second vs. 0.93 body lengths per second in the three-link swimmer).

Flexible swimmers also have the potential to perform back and forth movement. In theory, helical flagellar designs allow for back and forth movement through changing the direction of spin of the helix. However, in one tailed planar flagellar microrobots, moving in the opposite direction requires a U-turn which may be difficult to achieve in narrow vessels. This limits their use for tasks that require back and forth motion in such biological environments. To address this issue, Khalil et al. [69] reported a bidirectional flagellated actuation without the U-turn trajectory. This study looked into the change of direction on the same trajectory of a microrobot that possesses two flagella of unequal length and the effect of flagella lengths on reversal frequency (Fig. 6a). It proposes and attempts to verify a model that predicts velocity based on the tail length ratio and magnetic field frequency and determines the reversal frequency of the different length ratios tested. Five tail ratios were tested in a glycerine medium. Experimental results showed that the longer tail provided the greater propulsive force at frequencies below the reversal frequency and that the reversal frequency value increased with tail length

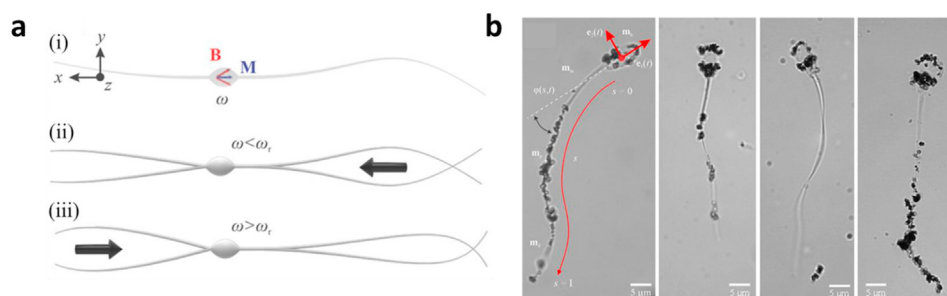


Fig. 6. Soft flexible magnetic micro/nanorobots. (a) A soft-bodied two-tailed microrobot with a magnetic head and two collinear, unequal, and opposite tails fabricated using electrospinning. (i) Magnetic particles are incorporated within the head to provide magnetization (m) and directional control under the influence of a periodic magnetic field (B) at frequency ω . (ii) Below reversal frequency (ω_r), the net propulsive force enables the microrobot to swim using its long tail. (iii) Above ω_r , the short tail allows for swimming along the opposite direction [69]. (b) Bovine sperm cells are coated with rice grain-shaped maghemite nanoparticles resulting in soft IRONSperms [25]. (All images used with permission). IRONSperm, iron oxide nanoparticles adhered to part of the surface of the entire sperm cell.

followed by the dissolution of the membrane in NaOH to release the swimmers. A set of triaxial Helmholtz coils were used to generate a rotating magnetic field for the actuation of the swimmer. Under the influence of a rotating magnetic field, the nickel head rotated causing the silver tail to deform in such a way as to produce a whipping motion resulting in the propulsion of the swimmer. The swimmer was used to transport spheres of sizes of 500 nm to 2.5 μm with the researchers noting that the particle size affected the speeds achieved by the swimmer. An interesting observation was the increase in speed when the swimmer carried particles of 1.25 μm compared with when it bore no load. Although the load of magnetic drug-containing particles increases viscous drag, it also sets up a rotating field because of spinning motion of these particles and, consequently, affects the propulsion speed of the nanoswimmer. Therefore, when the size of drug particles is approximately 1.25 μm , the speed of the nanoswimmer actually increased. However, further increase of the size of drug particles will lead to reduction of the speed of the nanoswimmer.

A concern for this design is how effective it will be in the treatment of tumors as nanowires are not likely to be readily taken up by cancer cells. There are also concerns about premature drug release; therefore, the researchers hope to investigate stronger attachment methods as well as stimuli responsive and specific release of the drug carrying nanoparticles. In addition, the means of propulsion needs to be verified as operable in flow environments similar to those found in many body fluid systems.

2.2.2. Helical swimmers

Helical- or screw-type microrobots and nanorobots are widely studied because of their proven propulsion abilities. However, many robots have been limited by their inability to be propelled in gels and other complex media such as the extracellular matrix (ECM). To further increase their use for biomedical applications, Schamel et al. [72] produced a 400-nm-long and 70-nm-diameter magnetic nanohelix capable of navigation through complex viscoelastic media. The nanohelix consists of a SiO_2 helix coated with a 40-nm-layer of nickel (for magnetic actuation by a rotating magnetic field) produced by the GLAD method [73]. Because of their small size (the smallest produced nanohelix at the time of publication), they have an advantage over their larger counterparts when moving through gels as they are similar in size to meshes in the gels. Although no movement of the nanohelix was observed in water because of Brownian motion, the dimensionless velocities achieved in gels were greater than the greatest of those achieved by microhelices in Newtonian fluid. The step-out frequency of the nanohelix was much higher than that of other micropropellers it was compared with, indicating a wider range of speed control of the nanohelices. This nanohelix shows potential in navigating complex fluid systems such as the ECM and, because of its small size, potential in being taken up by cells. Hence, further research can be done toward the determination of intracellular applications of such a nanorobot while also optimizing its design to prevent negative interactions with organelles and other cell components. In the study by Pal et al. [74], the irreversible trajectory was observed when they manipulated a helical nanorobot in a HeLa cell, which could be due to the influence of intracellular creeping flow and the reorganization of the intracellular matter. The study confirmed that the exquisite control of 250 nm nanorobots in cells is possible using rotating magnetic fields generated by a triaxial Helmholtz coil, despite the crowded intracellular environment.

2.2.3. Surface walkers

A more unique method of propulsion more recently being used in micro/nanorobots propulsion is surface walking. A recent example of a magnetically actuated microsurface walker is the Janus microdimer surface walker, consisting of two Ni/ SiO_2 Janus spheres joined magnetically [75]. Under the influence of a planar oscillating magnetic field and near a surface, the spheres roll over each other in an asymmetric fashion that results in the net displacement. This is different from both propulsion methods discussed in Section 2.2.1, 2.2.2 earlier as it does not

involve a swimming type of motion. This method opens up new prospects in the field of micro/nanorobot propulsion, especially in confined spaces and complex geometries. Because of this device's robust navigational ability and its efficiency in changing speed, the developers of this device envision it being applied to a wide range of uses from nanomanipulation to precise medical treatment. The actuation and operation of this device is further discussed in section 3.1.4.

2.3. Propulsion designs incorporating biological and synthetic components

Nature is a rich database which often inspires the ideas of scientists and can provide solutions to scientific challenges. There have been plenty of micro/nanorobot designs adapted from nature with research showing promising results for their applications in the biomedical area, for example, the adaptation of bacterial flagella [76]. Because of such findings, researchers attempted to preserve the original function of biological components and include them in their robot designs.

Ali et al. [77] created a self-assembled magnetic nanorobot consisting of bacterial flagella attached to a superparamagnetic particle for actuation and steering under a rotating magnetic field. To make the robots, flagella were obtained from *Salmonella typhimurium*, depolymerized into the constituent protein flagellin and then polymerized into flagella fragments of roughly equal length (200 nm) (Fig. 7a). The fragments were biotinylated using a method described by Asakura et al. [80] and Asakura and Iino [81], and the superparamagnetic particles of radii 40–400 nm were coated with streptavidin and placed in solution along with biotinylated flagella and agitated resulting in the attachment of flagella to particles [80,81]. To imitate environmental stimuli that results in conformational change, the swimmers were submerged in aqueous solutions containing organic solvents resulting in rapid conformational change, similar to actual bacteria. The use of these robots has the potential to overcome several limitations faced in *in vivo* biomedical applications of magnetic nanorobots. Flagella that change conformation in response to environmental stimuli would be beneficial in navigating the heterogeneous fluids which may present a physical barrier to robot navigation. Another benefit of this design is the simplicity of its fabrication process compared with several others that use complicated methods such as electrodeposition. Its fabrication method allows for easy batch production of robots of different flagella and particle sizes.

Beyond serving as a source of inspiration for sophisticated structures, incorporating natural organisms into micro/nanorobots entails many functional advantages, such as selective cytotoxicity, hydrophobicity/hydrophilicity, fracture resistance, facile uptake of therapeutic agents, autofluorescence, renewability, and biodegradability. Incorporating these interesting functionalities in magnetic robot fabrication could expand their biological applications.

Yan et al. [78] discovered that *Spirulina platensis*, a helical microalgae subspecies, exhibits intrinsic fluorescence, selective cytotoxicity to cancer cells and natural degradability. Attaching Fe_3O_4 nanoparticles on *S. platensis* surface via a dip-coating method results in magnetic microrobots under the general name magnetized *Spirulina* (MSP) which can be propelled by a rotating magnetic field provided by a tri-axial Helmholtz coil system and can perform *in vivo* imaging-guided therapy with an emission peak at around 650 nm (Fig. 7b). The microrobots were injected in the intraperitoneal cavity of nude mice to test their *in vivo* fluorescent imaging abilities. The results showed that MSP can stably emit fluorescent signals in mice for about 15 h.

Recently, Yan et al. [82] updated their MSP microrobots and applied them in controlled drug delivery. Apart from aforementioned beneficial features, *Spirulina* cells have large pores for slime secretion allowing for the uptake of large molecules. Thus, in this study, they used the dehydration and rehydration of spirulina for molecular loading. The spirulina microrobots were successfully navigated through a fluidic channel modeled after the intestinal tract containing intestinal fluids demonstrating precise control capabilities. The loaded molecules were released because of two mechanisms, namely concentration gradients and

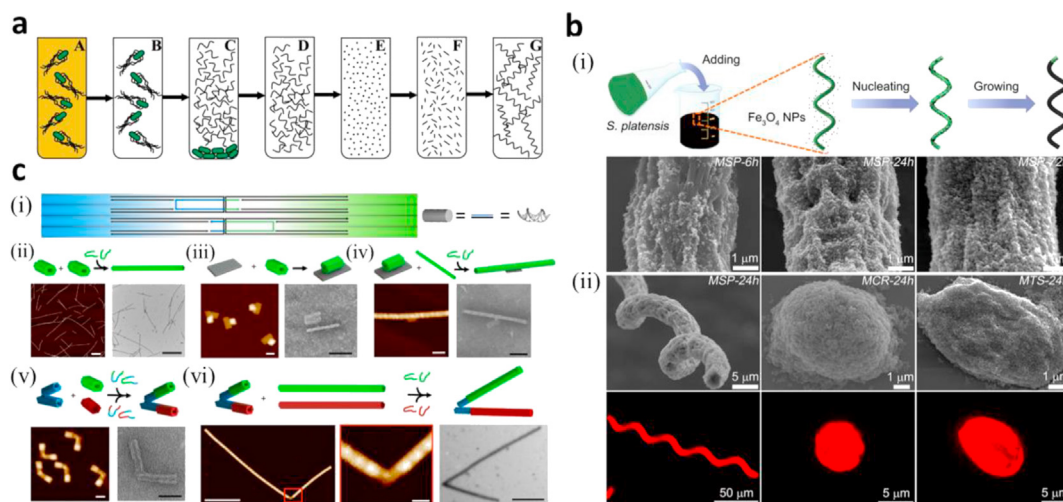


Fig. 7. Micro/nanorobots involving biological components. (a) The diagram of flagella repolymerization [77]. (b) Magnetized Spirulina. (i) The schematic of the dip-coating process of *S. platensis* in a suspension of Fe_3O_4 NPs. (ii) FESEM (top) and fluorescence images (bottom) of MSP-24 h, MCR-24 h, and MTS-24 h samples [78]. (c) Assembly of DNA origami micromachine systems. (i) The ssDNA connecting two structures (polymerization strands) were designed with a U-shaped motif, where half have a higher affinity to attach to one side of the interface whereas the other half have higher affinity to the other side of the interface. (ii) Stiff microlevers are assembled by attaching 56 helix nanobricks end-to-end using polymerization strands. AFM and TEM images show microlevers. The scale bar is 1 μm . (iii) The nanorotor is assembled by attaching a nanoplatform to a nanobrick via a single ssDNA overhang. AFM and TEM images show the nanorotor construct. The scale bar is 50 nm. (iv) Stiff microlevers are formed off the arm of the nanorotor using polymerization strands to connect the nano-arm to microlevers. AFM and TEM images show the hinge with top and bottom nanobricks attached. The scale bar is 50 nm. (v) A single nanobrick is attached initially to the top and bottom of the nano-hinge using two separate sets of polymerization strands for top (green-blue) and bottom (red-blue). AFM and TEM images show the hinge with top and bottom nanobricks attached. The scale bar is 50 nm. (vi) Stiff microlevers are formed off the initial nanobricks by attaching top nanorods (green) and bottom nanorods (red) using two separate sets of polymerization staples for the top (green) and the bottom (red). The zoomed out image of AFM and TEM images show a polymerized nano-hinge (Scale bars are 500 nm, left and right). The zoomed-in image of the nano-hinge from in the AFM image (The scale bar is 50 nm, middle) [79]. (All images are used with permission). FESEM, Field-emission Scanning Electron Microscopy; AFM, Atomic Force Microscopy; TEM, Transmission Electron Microscopy.

spirulina degradation, with more molecules released the longer the residence time. The release of molecules from these transporters can be controlled by adjusting magnetite thickness with thicker coatings showing a slower rate of molecule release. This method of control, however, requires a good knowledge of the amount of time it would take to navigate to targets which will be difficult in a system as complex as the gastrointestinal system. External stimuli could be investigated as an alternative means of controlling molecule release.

Another significant advantage of biological components is their biocompatibility, with particular regard to components originating from within organisms, for example, various immune cells, DNA, sperms, and plasma cells.

A good example is the macrophage, an immune cell which may also have tumor targeting properties making it beneficial for chemotherapeutic purposes as they could allow for better targeted drug transport, potentially reducing the effect of such therapy on healthy tissues and cells. In the work by Han et al. [59], a hybrid-targeting method based on magnetic actuation and the propensity of macrophages to gather around solid tumors is proposed for more efficient targeting. This microrobot consists of poly-lactic-co-glycolic-acid (PLGA) spheres containing magnetic and chemotherapeutic nanoparticles which are taken up by phagocytotic macrophages. The microrobots are actuated using a gradient magnetic field generated by three Helmholtz coils and Maxwell coils and their motion controlled by adjusting coils' currents. The microrobots brought into the vicinity of tumor spheroids were found to infiltrate into them because of macrophage recruitment. This microrobot design was further modified using liposomes in place of PLGA for MNPs and drug containment as well as near-infrared (NIR) radiation stimulated enhanced drug release [83]. Similarly, the robots were made by phagocytosis of liposomes containing MNPs and taxol (anticancer drug) prepared by thin-film hydration [84]. NIR radiation enhanced the drug release rate because of the temperature sensitivity of one of the liposomes' components causing a phase transition, effectively melting the

liposome and releasing the drug when exposed to NIR. Further work is desired to refine this design by conducting tests in animals involving the extraction of macrophages from different organs and identifying the best to use for investigations with a final goal of being able to implement this treatment method in humans with cancer [59].

DNA origami structures have gained a lot of attention in the nanotechnology field because of their potential to be used as building blocks for nanoscale machinery [85,86]. Lauback et al. [79] presented a set of microdevices assembled from nanoscale DNA origami structures, actuated by magnetic fields with subsecond response times. The first device is a nanorotor, capable of continuous rotational motion, and the second device is a nano-hinge capable of limited relative rotational motion (angle of about 120° between the 2 arms). The actuation of these structures is due to the magnetic torque experienced by the magnetic microsphere when a rotating magnetic field is applied. The arms used in these structures consist of bricks as in Fig. 7c formed from multiple DNA double helices. The rotor was able to execute 120 complete continuous rotations, and both structures are able to hold different conformations with precision of about 8° . The study mainly explored the magnetic actuation of DNA origami structures; hence, no testing for biomedical applications was done, although it was suggested that these structures could be used in the field of protein engineering for enzyme control and other applications. A major benefit of these structures is the low cost of making the control system which can be assembled from cheap electromagnets, increasing this design's potential for commercial availability.

Sperms are naturally adapted to swim in the female reproductive environment, and a study found that sperms can display a high uptake of doxorubicin hydrochloride (DOX-HCl) (a hydrophilic anticancer drug) because DOX-HCl exhibits high-binding affinity to DNA (nucleus) [87]. Based on this, to design a drug-loading microrobot for targeted cancer treatment, Magdanz et al. [25] adopted bovine sperm cells (length of $\sim 60 \mu\text{m}$) as the temple to fabricate soft magnetic microrobots via a simple electrostatic-based method (Fig.6b). Because of opposite surface

zeta potentials, iron oxide nanoparticles adhered to part of the surface of entire sperm cells (IRONsperms), which ensures magnetically actuated helical flagellar propulsion while flexibility. Their results displayed that the moving speed of IRONSperms can exceed $6.8 \pm 4.1 \mu\text{m/s}$ under a rotating magnetic field actuation with a frequency of 8 Hz. After coculture of IRONSperms and DOX-HCl for about 1 h, IRONSperms showed good cargo-encapsulating ability with $4.3 \pm 0.2 \text{ pg}$ of DOX-HCl per IRONSperm.

Often when operating *in vivo*, small-scale robots are attacked by the body's immune system or bound to biological molecules. Although substantial research has been done into the development of more biocompatible microrobots and nanorobots, most have a focus on reducing cytotoxicity and negative effects which these devices have on biological systems, but little has been accomplished in research on the reduction of interactions that are detrimental to the performance of these devices. Because of this, Li et al. [88] developed a helical nanoswimmer coated with the plasma membrane of human platelets to allow for hindrance-free propulsion by avoiding biofouling. Human platelets have many functions in the blood, for example, immune evasion, pathogen interactions, and subendothelium adhesion [89,90]. These also give the nanoswimmer-added functionality due to the ability to specifically bind certain substances. The fabrication of these swimmers involves electrochemical deposition of palladium into a template followed by dissolution of the template in methylene chloride to release the swimmers. The swimmers are then coated in nickel (for magnetic actuation) and gold by electron beam evaporation. A negative charge is induced on the gold surface by incubating the coated swimmers with 3-mercaptopropionic acid. After incubation with plasma membrane vesicles, the protein coating is adsorbed onto the gold surface. The protein-coated swimmers displayed much greater propulsion speeds than uncoated swimmers when tested in plasma, serum, and whole blood exemplifying their enhanced performance in biological media. The swimmers further demonstrated their abilities by maintaining propulsion speeds after incubation with blood indicating little or no biofouling. During experimentation, it was also noted that some toxins and pathogens selectively bound to the surface of the swimmer as they would to platelets, diverting the pathogens away from healthy cells [90]. The swimmer was able to bind to up to 15 bacteria at a time indicating its potential to be used as a means of pathogen diversion from healthy cells. The study envisions further development of this design leading to it becoming a new standard method of pathogen isolation and diversion.

Beyond directly employing natural biological components to fabricate micro/nanorobots, it is also common to create such systems to simulate the nature. For instance, a behavior which has been adapted from nature recently is the swarming behavior observed in some insects, birds, and fish. The ribbon-like paramagnetic nanoparticle swarm by Yu et al. [91] consists of paramagnetic nanoparticles reconfigured into microstructures termed microswarms using oscillating magnetic fields. This design is advantageous because of its ability to elongate reversibly and greatly increase its aspect ratio, split into subswarms, and navigate multiple channels simultaneously and other abilities. The ability of the microswarms to maintain stability when encountering obstacles was demonstrated by navigating the device to approach solid boundaries of different geometries including circular, planar, and sharp-angled boundaries. After these tests, the microswarms maintained their shape and only lost a few nanoparticles. The microswarms also demonstrated its non-contact ability to manipulate other microstructures by arranging randomly distributed polystyrene microbeads into a straight line. The envisioned biomedical applications of this device include targeted delivery and micromanipulation.

Another example is an artificial soft magnetic cilia carpet fabricated by Gu et al. [92] which can vividly mimic the walking of the millipede. Xie et al. [93] designed a spheroidal soft hydrogel microrobot embedded with a chain of aligned iron oxide nanoparticles inside which can precisely mimic the flexible motion of magnetotactic bacteria. This soft microrobot is capable of working in confined biomicroenvironment such

as vessels, resulting in great promise in microvascular thrombolysis and ultramini-mal invasive surgery.

2.4. Multifunctionality in magnetic micro/nanorobots

2.4.1. Hybrid actuation

Several recent designs of small-scale robots consist of various functional materials that let the magnetic robots respond to more than one type of external stimuli (e.g. light, ultrasound, and temperature), resulting in hybrid actuation and multifunctionality. As concluded in a recent review, magnetically and optically actuated microrobots have different pros and cons in material, locomotion performance, or biocompatibility [94]. Magnetic microrobots are more promising for applications in deep tissue because of better locomotion and navigation and optical microrobots are softer and more suitable working in transparent environments or used for biotechnology and lab-/organ-on-a-chip. Therefore, naturally, the combination of these two actuations may potentially combine their advantages. Similarly, the combination of other actuation will be beneficial as well.

Low-frequency ultrasound waves have the potential ability to aid in guiding the movement of magnetic robots because of their deep penetration *in vivo*. Khalil et al. [95] developed a magnetic helical microrobot used for the mechanical disruption of blood clots, which was actuated by rotating magnetic fields and tracked by an ultrasound system. The ultrasonic field they produced has a maximum penetration depth of 16 cm and can locate the microrobots via their ultrasound feedback and guide microrobots toward blood clots. After arriving at the blood clot area, the rotating magnetic fields induce a rotary motion in the helical microrobots at $\omega = 35 \text{ Hz}$ to rub against and tear the fibrin network of the clot. At body temperature, using this rotary frequency, these microrobots have a blood clot cleaning rate of $-0.482 \pm 0.23 \text{ mm}^3/\text{min}$. Combining acoustic actuation with rotational magnetic actuation, Ahmed et al. [46] reported a special propulsive mechanism which can let magnetic spheroidal aggregates perform a rolling motion along vessel walls. Acoustic fields of appropriate frequencies can force magnetic aggregates to migrate to the vascular boundary (Fig. 8a). This close-to-wall propulsive mechanism could eliminate the thrombosis caused by the shear-induced platelet activation resulting from the rolling motion of microrobots.

The sperm-templated soft magnetic microrobots described in Section 2.3 were also one example of hybrid actuation [25]. The localization of IRONSperms was achieved by ultrasound waves because the coated iron oxide particles enhance the acoustic impedance of IRONSperms. The study displayed that only a 20-MHz ultrasound wave can visualize a single IRONSperm *in vitro*.

Chen et al. [96] reported a magnetically actuated helical piezoelectric microrobot made up of a polyvinylidene fluoride-co-trifluoroethylene (P(VDF-TrFE)) matrix encasing MNPs applied in targeted cell delivery. This microrobot is used to ultrasonically stimulate cell differentiation for neural networks repair. The piezoelectric microrobots are loaded with neuron-like cells which differentiate because of the electrical polarization of the piezoelectric body when exposed to acoustic waves (Fig. 8b, i-ii). These microrobots are manipulated by a rotating magnetic field causing them to swim in a programmed corkscrew motion to the targeted area. The fabrication of the microrobots involves mixing CoFe_2O_4 MNPs into a piezoelectric polymer solution ensuring even distribution of the particles. A copper wire of the desired helical diameter is coated in the mixture, and a moving laser is used to cut the coating into the desired helical shape and pitch. The microswimmer is then released from the copper wire by selective etching. As the machine is intended to work in the brain, the suitability of the robot for working in the environment of the ECM (of typical viscosity around 200 mPas) was assessed by testing it in silicon oil with a viscosity of 340 mPas. One swimmer, optimized in terms of the pitch angle, length, and etch ratio achieved a top speed of 0.5 mm/s at a magnetic field frequency of 5 Hz in silicon oil. The swimmer was able to move in three dimensions, however, only until a frequency of 1.8 Hz. To test the swimmers' ability to induce cell

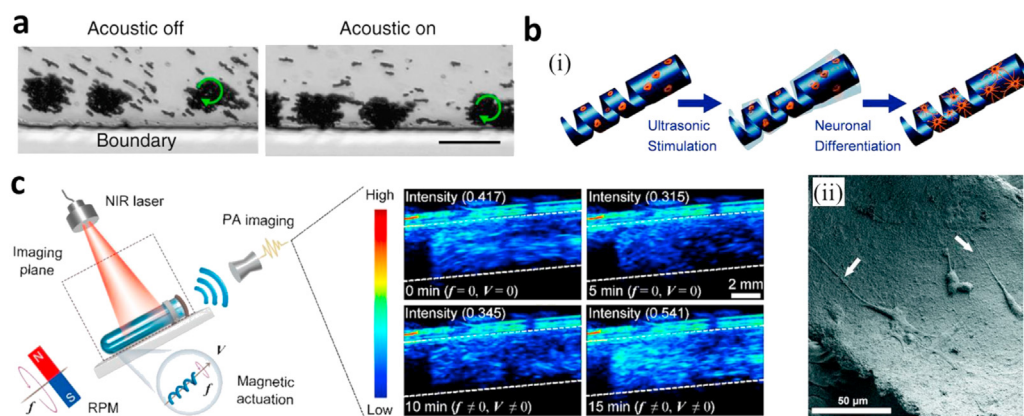


Fig. 8. Micro/nanorobots with hybrid actuations. (a) Rolling motion in acoustic and magnetic fields. The aggregate migrates toward the channel wall because of the radiation force of an acoustic field [46]. (b) (i) Schematic illustration: ultrasound (US) stimulation of the piezoelectric microswimmer induces neuronal differentiation of PC12 cells. (ii) An SEM image showing differentiated PC12 cells on the inner surface of a helical swimmer after US stimulation [96]. (c) NIR laser induced photothermal therapy and PA image tracking ability in a plastic tube [60]. (All images are used with permission). SEM, Scanning Electron Microscopy; NIR, near-infrared.

differentiation, the swimmers were put under acoustic stimulation with cell differentiation clearly observed after 7 days.

Polydopamine (PDA) as a functional coating has attracted much attention in the biomedical field over the last decade because of its versatile characteristics. These characteristics include the ability to adhere to almost all materials, strong NIR absorption, biodegradability, and excellent water solubility [97–99]. Xie et al. [60] used PDA to coat MSP microrobots designed by Yan et al. [78] to give them more functions. This coating allowed for the photothermal therapy and photoacoustic imaging of the MSP microrobots as PDA can generate photothermal effects and strong photoacoustic signals under NIR laser irradiation (Fig. 8c). In this study, the corkscrew magnetic actuation was provided by a commercial system (MFG-100-I, MagnebotiX, Switzerland) (Fig. 4).

When the body of a soft micro/nanorobot consists of thermoresponsive hydrogels, for example, the microrobot designed by Iacovacci et al. [100], MNPs inside the microrobot can not only actuate the locomotion, but also induce the shape transformation (tubular to planar) of robots under the magnetic field. This morphological change can be used for controlled drug delivery and release. Another work by Go et al. [101] presented a similar magnetically actuated microrobot that can fold and unfold in response to temperature changes. The microrobot is made up of layers of polyethyleneglycol diacrylate loaded with MNPs for magnetic actuation and N-isopropylacrylamide (NIPAM) which is sensitive to temperature. Upon heating, NIPAM releases water and shrinks. Coupling this shrinking to a stable structure results in the folding of the microrobot into a spherical cage-like structure. The folding and unfolding properties allow for this microrobot to pick up, transport, and release therapeutic agents. Magnetic actuation was done by an EMA system consisting of three Helmholtz coils for propulsion and two Maxwell coils for navigation. The device was successfully navigated toward a microbead containing therapeutic agents, positioned near it, and heated to induce folding resulting in the entrapment of the microbead. The device used the rolling motion to deliver the microbead to the desired site and was then cooled allowing for the release of the microbead. One device could transport up to five microbeads at a time, and the delivered microbeads demonstrated their therapeutic effect by severely changing the morphology of cancer cells that were cultured with for 24 h. Moving forward, this design could be adapted at nanoscale to allow for wider use.

2.4.2. Uses of magnetic field to induce local non-magnetic effects

Although hybrid stimuli are often used to achieve multifunctionality, the interactions of diverse magnetic fields with different materials can also produce different responses such as deformation in magnetostrictive materials and imaging in some other materials. This implies that micro/nanorobot multifunctionality under one type of the external stimulus (magnetic field) can be achieved.

Chen et al. [102], the same group that produced piezoelectric microrobots (in Section 2.4.1), used the same polymer (P(VDF-TrFE)) along with magnetostrictive iron–gallium (FeGa) alloys as the functional materials to manufacture a nanoscale wire-shaped magnetic robot. The combination of these materials in the robot allows for the spontaneous electric polarization of P(VDF-TrFE) resulting from its strain which is termed the piezoelectric effect. Thus, these materials enable both targeted drug delivery and release under only magnetic field stimulation. Fabrication of these nanorobots first involves the formation of P(VDF-TrFE) nanotubes using a template-based wetting method. This is followed by electrodeposition of the FeGa alloy into the tubes. PDA is then adsorbed onto the surface of the produced nanotubes to allow for drug binding. Under the influence of an alternating magnetic field, the magnetostrictive core deforms producing strain which triggers a piezoelectric response in the shell, redistributing the charges on its surface. This results in the breaking of the bonds between the PDA and the drugs resulting in their release (Fig. 9a). This nanorobot is unique in that it is rigid and can execute 3D motion via an unsymmetrical rotary motion, which traces out a cone shape when it is actuated using a cone-shaped rotational magnetic field. Under a rotating magnetic field, it moves via a tumbling motion. The drug-release method presented here was verified by navigating the robot to cancer cells and triggering the magnetoelectric effect which resulted in a 40% drop in the viability of the cancer cells. It was also observed that there was negligible drug release under direct current (DC) fields used for navigation.

Recently, this group also produced a similar piezoelectric wire-shaped nanorobot named ‘nanoeel’, this time, removing the alloy core resulting in a soft polymeric body [103]. This soft piezoelectric ‘nanoeel’ is still capable of magnetic actuation and controlled release of drugs, and magnetic fields worked as the single external power source as well. The nanoeel consists of a nickel head for magnetic actuation and a flexible piezoelectric P(VDF-TrFE) tail linked by a polypyrrole nanowire. Fabrication was done using the coaxial lithography technique, involving the deposition of the constituent materials of the nanoeels into an anodized aluminum oxide membrane template [104]. The drugs were functionalized on to the surface of the nanoeels by subsequently dispersing the nanoeels in solutions of Tris-HCl, dopamine, and RhB (drug). Under alternating magnetic fields, the flexure of the soft P(VDF-TrFE) tail was induced resulting in a change in its electric polarization leading to desorption of drugs loaded on the surface of the tail (Fig. 9b). Results showed that about 90% of the drugs were released under the induced piezoelectric effect, compared with a negligible amount without piezoelectric stimulation. The therapeutic effect of this design was also improved under piezoelectric stimulation with 35% of cancer cells killed under stimulation compared with 10% without. Betal et al. [105] designed a magnetoelectric nanorobot which also utilizes the piezoelectric effect and is capable of the targeting, permeation, and transport

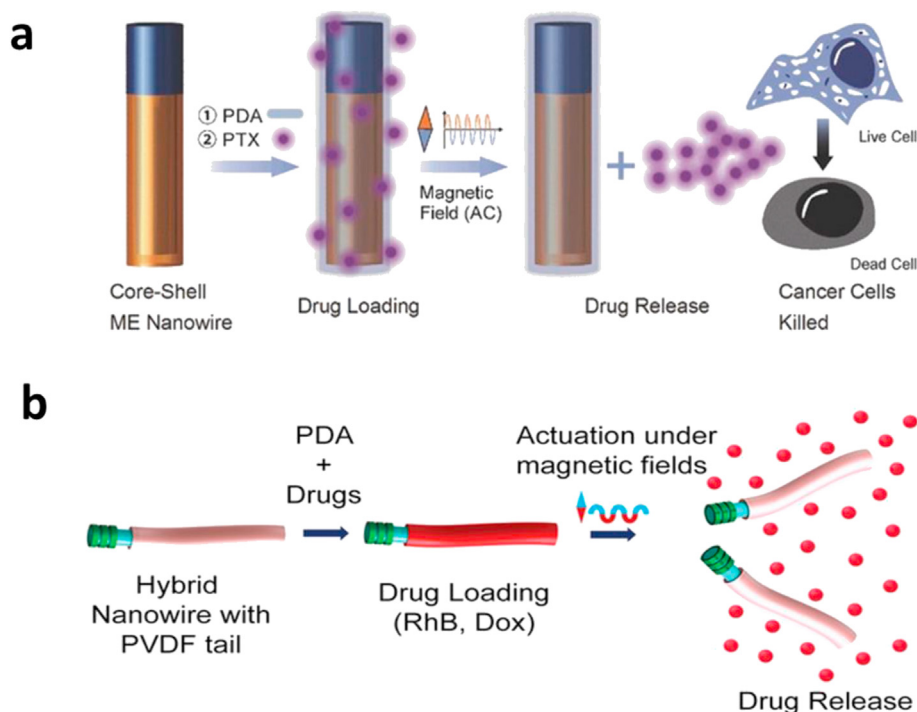


Fig. 9. Magnetic fields induced non-magnetic effects. (a) FeGa@P(VDF-TrFE) core-shell nanowires. The anticancer drug is loaded onto a PDA-treated FeGa@P(VDF-TrFE) core-shell nanowire and then released by applying an alternating magnetic field. [102]. (b) A soft hybrid nanowire with PDA and drugs, followed by magnetically triggered drug release [103]. (All images are used with permission). Dox, doxorubicin; RhB, rhodamine-B; ME, magnetolectric; AC, alternating current; PDA, polydopamine; PTX, paclitaxel; P(VDF-TrFE), polyvinylidene fluoride-co-trifluoroethylene.

of living cells. This nanorobot consisted of a magnetostrictive CoFe_2O_4 core and piezoelectric BaTiO_3 shell and was controlled by alternating current (AC) and DC magnetic fields. Under a DC magnetic field of -50 Oe, the piezoelectric effect gave rise to negative and positive dipoles on the device's shell. The negative dipole repelled the negative cell membrane resulting in thrust generation which could be used to propel cells until obstacles were encountered or the magnetic field was turned off. For cell-targeting purposes, a 40 Oe, 30 Hz AC magnetic field caused the nanorobot to produce low-intensity negative pulses just strong enough to create a repulsive force. This resulted in the motion of the nanorobot and subsequent avoidance of other negatively charged obstacles. This interaction also resulted in increased propulsion speeds in high-cell-density

areas. To permeate cells, the nanorobot was excited under a 50 Oe, 60 Hz AC magnetic field. This induced magnetostriction in the core which when coupled with piezoelectric nature of the shell produces a negative pulse strong enough to temporarily dislocate the phospholipid layer of the cell membrane when close to cells. This work has provided a novel means of cell manipulation, combining multiple functionalities typically performed by different tools into a single device. This allows for minimally invasive cell therapy, cell engineering, and more. However, its current fabrication methods are very complex and energy intensive; thus, this can be investigated further to develop a more cost-effective manufacturing technique leading to this device's commercial availability and use.

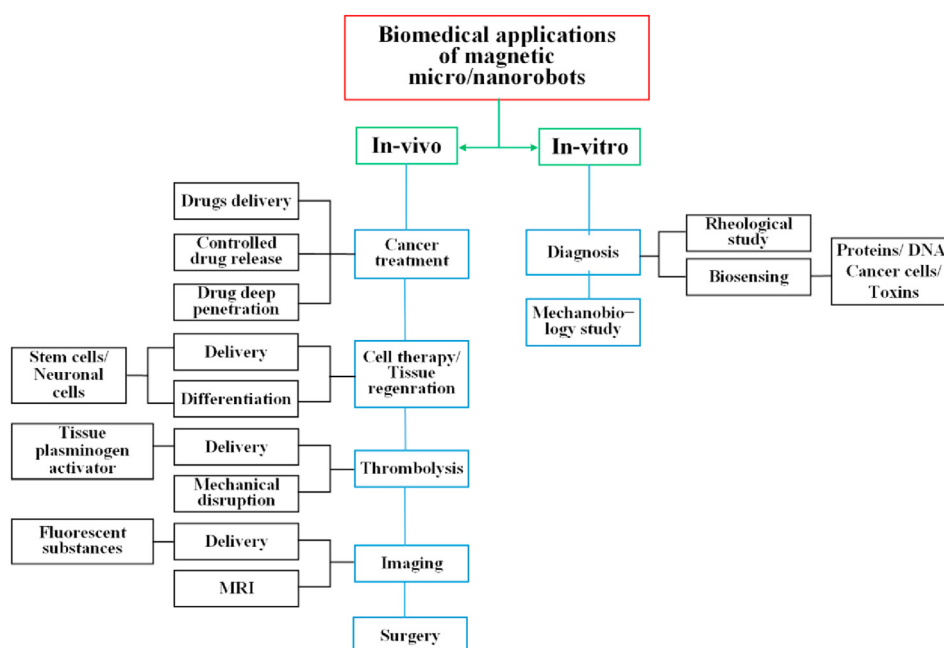


Fig. 10. The biomedical applications of magnetic micro/nanorobots. MRI, magnetic resonance imaging.

3. The biomedical applications of magnetic micro/nanorobots and the process toward clinical use

3.1. *In vivo* and *in vitro* biomedical applications

The current biomedical applications of micro/nanorobots are summarized in Fig. 10. They can be classified into two broad categories in this review, *in vivo* and *in vitro* applications. As described in the previous content, some magnetic robots focus on one application, but some devices can perform multiple functions.

3.1.1. *In vivo*: cargo transport and enhanced therapy

One of the most significant functions of micro/nanorobots is transportation because of their precise active movement and relatively high speed to the targeted areas compared with passive diffusion. As delivery devices, they can achieve a number of diverse applications depending on their loaded cargos. For example, they can be used for cancer treatment when their cargos are anticancer drugs; they can deliver live cells for cell therapy, deliver tissue plasminogen activator for thrombolytic purposes, and deliver fluorescence agents for *in vivo* imaging [60,106–108].

To transport cargos, Lee et al. [109] fabricated a microrobot with a capsule-like head. This capsule-like head can capture drug-loaded particles and suspended or adherent cells, then assemble with the cap to encapsulate cargos, and deliver them to the targeted area via a corkscrewing motion under rotating magnetic fields. This microrobot comprised a magnetic helical plunger produced by 3D laser lithography and physical vapor deposition of Ni and Ti layers and a cap. To unload cargos, an opposite rotating field was provided to open the cap. The maximum translational velocity of this helical microrobot was $850 \mu\text{m s}^{-1}$ achieved under 10 mT at 65 Hz. Recently, this group used the same fabrication method to produce another similar helical microrobot in which the capsule-like head was replaced by a needle-like structure that can stab the targeted tissue [110]. Thus, this type of magnetic microrobot can be fixed at lesion tissues preventing the flushing away of the microrobots by body fluids without the magnetic actuation assistance. This enables the long-term release of drugs from microrobots for efficient therapy.

Apart from the targeted delivery of therapeutic agents to the tumor areas and their controlled release (Many studies on this have been discussed in previous sections), magnetic microrobots can also facilitate the deep interstitial penetration of these agents in solid tumors to maximize their therapeutic efficiency. Tumor tissues normally have high interstitial pressure which will prevent the diffusive transport of drugs that are released from robots [111]. Schuerle et al. [112] studied two magnetic microrobots which used two different strategies to induce the localized convective flow for enhancing tissue penetration of nanoparticles. One is the helical-like artificial bacterial flagellum (ABF), and the other one is the natural magnetotactic bacteria (MTB) with two chains of magnetic crystals inside. Under the actuation of a 3D uniform rotating magnetic field consisting of eight electromagnets, the ABF will disrupt laminar flow via their rotational forward motion, which can force nanoparticles to move toward the vascular wall and penetrate into the adjacent tissues. In contrast, dense swarms of MTB can generate volumetric convective flow via their circular motions under the same magnetic field. Combining their tumor-homing properties, they were observed to penetrate tumor ECM and induce convection, further increasing the penetration of nanoparticles in tumor.

Intravitreal microrobots and nanorobots have been envisioned to be of great use in ocular therapies and procedures. This is partly due to the relative ease of visualization of such devices in the eye compared with other parts of the body, but also due to the challenges faced in the use of topical and other therapies currently used in ophthalmology. Two major challenges faced in the use of intravitreal microrobots or nanorobots are the difficulty of propelling through the vitreous humor because of adhesion and its tight matrix which prevents penetration. Considering this, Wu et al. [113] presented magnetically actuated helical

micropropellers sized to efficiently propel and navigate through the matrix of the vitreous humor. These micropropellers were also given an additional liquid layer coating allowing the device to overcome adhesive forces. These microhelices were made of SiO₂-Ni using the GLAD technique. The researchers noted that because Ni is toxic, Fe can alternatively be used as the magnetic component with very similar performance to improve biocompatibility. The micropropeller was able to navigate from the center of the vitreous membrane to the retina in 30 min, about ten times as fast as passive diffusion of a similarly sized particle. The researchers, therefore, envision this device as a means of targeted delivery, significantly reducing the amount of time it takes for certain therapies to work and reducing the side effects caused by the non-specificity of passive diffusion. The researchers proposed that this device's precision in targeted therapy could be improved with a controlled injection system and instantaneous feedback and navigation of the micropropeller through the vitreous humor.

The potential to use MRI machines for targeted therapy termed magnetic resonance targeting (MRT) has also been explored by research groups. A study by Muthana et al. [114] detailed the successful navigation of magnetic macrophages from the blood stream into tumor sites in mice using an MRI system operating at 300 mT. This enhances therapy by increasing the infiltration of the tumor by macrophages. The MRI system also allowed for the imaging of macrophage distribution after MRT alluding to the potential of real-time imaging for navigation purposes. The researchers envision this technology being used for targeting tumors and other cell types such as mesenchymal stem cells.

At present, most magnetic robots designed for *in vivo* applications have only been verified on *in vitro* models (e.g. microfluidic system) or *ex vivo* models, with only few of them passing to the animal tests [115–117]. This may be due to the resource restrictions for large magnetic fields set up, the difficulty in *in vivo* observation of the robots, and most robots' inability to deal with realistic medical environments of complex geometry filled with biological fluids. Notwithstanding, highly qualified *in vitro* proof-of-concept studies are solid foundations for progressing to *in vivo* verification. Table 1 lists the current publications that contain *in vivo* tests. It can be seen that although these robot models have been tested on animals, they were mainly subcutaneously injected into the diseased areas or intraperitoneal cavity for imaging experiments.

3.1.2. *In vivo*: surgery

Magnetically manipulated micro/nanorobots have promising application in minimally invasive surgery because magnetic fields have natural ability to penetrate thick biological tissues. In a new study, Vyskočil et al. [40] reported the possibility of magnetic microrobots performing microsurgery in cancer cells. They fabricated a rod-shaped 'walking' Au/Ag/Ni microrobotic scalpel via sequential electrodeposition of these three elements into commercial polycarbonate membrane holes after an H₂O₂ etching step to partially remove the middle Ag segment (Fig. 11). The length of microrobots is about 6 μm and 600 nm in diameter. Because of the magnetic asymmetry of microrobots (one Ni end) and the bent Ag part, the microrobot can transversally move and enter in human osteosarcoma (U-2 OS) cells under a weak transversal rotating magnetic field (5 Hz at 3 mT). They estimated that under this magnetic field conditions the microrobots are capable of generating force up to 100 pN. As a result, they observed that the microrobotic scalpel can move in the cytoplasm, extract a small cellular fragment, and then remove it outside the cell.

As surgical operation requires various tools to grasp and remove diseased tissues, the minimally invasive surgery also needs miniaturized tools for precise surgery. Thus, the demand for developing precisely controlled small-scale tweezers or grippers is increasing [119–122]. Barbot et al. [123] fabricated a magnetic sheet by curing the mixture of polydimethylsiloxane (PDMS) and iron powder, and then the sheet was cut into rectangular microrobots (2 mm-3mm-200 μm) which enabled floating on a fiber for wet transfer. Two of these microrobots with different preferred magnetization directions (different iron line directions) can form a gripper and grasp the item between them under the

Table 1
Publications including *in vivo* experiments of magnetic micro/nanorobots.

Shape of robots	Type of magnetic fields	Applications	<i>In vivo</i> models	Administration methods	Reference
Helical Rod	Rotating	Imaging	Mice	Intraperitoneal injection	2017 [78]
	Rotating	Targeted thrombolysis	Distal middle cerebral artery occlusion mouse model	Internal carotid artery injection	2018 [108]
Porous spheroid	Gradient	Cell delivery/release	Yolks of zebrafish embryos/mice	Injection/subcutaneous injection	2018 [115]
Helical	Rotating	Imaging/photothermal Antibacterial Therapy	Mice	Subcutaneous injection	2020 [60]
Helical	Gradient	Cancer imaging Radio-Photodynamic Therapy	Mice	Intravenous injection	2020 [118]

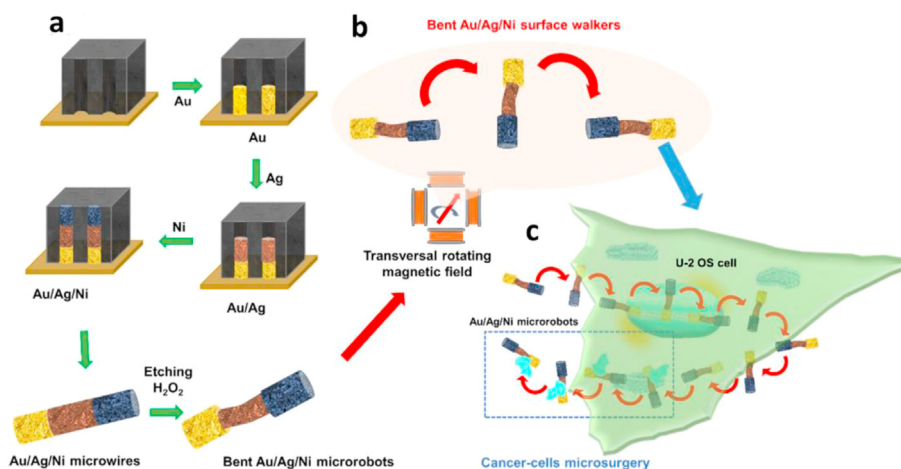


Fig. 11. Microrobotic scalpels. a) Surface microrobotic scalpels fabrication by sequential electrodeposition of Au, Ag, and Ni into polycarbonate membrane holes and b) Au/Ag/Ni surface microrobotic scalpels motion in a transversal rotating magnetic field and c) its application for cancer cell microsurgery [40]. (All images are used with permission). PVA, polyvinyl alcohol.

control of a permanent magnet. The microgripper can generate the average force of 0.5 N, its transfer precision is within 5 μm , and the orientation error is lower than 0.4°.

Vascular diseases have been identified as a disease that is becoming more widespread nowadays because of recent prevalent lifestyles. The invasiveness and side effects of current treatment methods have led researchers to search for alternatives. Previous studies have shown the potential of magnetic microrobots capable of drilling through thrombi as a possible treatment for thrombosis; however, most of these designs have only been tested in 2D environments where the effects of gravity do not need to be taken into account. To evaluate the potential of using this design in 3D space, which better emulates the human cardiovascular system, Lee et al. [124] developed and tested a magnetic drilling actuator (MDA) capable of 3D navigation. This device consists of a 3D printed drill made of MicroFine, an acrylonitrile butadiene styrene-like material with a neodymium alloy insert for magnetic manipulation. The MDA is actuated using an EMA system (Octomag, Aeon Scientific GmbH, Switzerland), consisting of eight hemispherically configured electromagnetic coils with different currents flowing through them. Three different designs with two, three, and four spirals were tested in a vascular network mimicking fluidic channels to determine which was best for optimal drilling and propulsion. The MDA was able to accurately navigate and drill through an artificial thrombosis made of gelatine and porcine blood to mimic soft jelly-like thrombi. As the MDA is remotely controlled and capable of robust 3D navigation, it can simply change direction to drill through thrombi multiple times if the need should arise. The researchers suggest that this device can be visualized using X-ray or CT scans and intravascular ultrasound. Although the MDA is not at the microscale, this research presents a crucial step toward the use of microscale devices similar to the MDA in the complicated network of the

cardiovascular system.

3.1.3. Rheology and biosensing

Rheology, the study of flow is of great importance in several fields, particularly in the biological/biomedical field where there can be striking differences in fluid properties depending on length scale of investigation. Jeong et al. [6] presented a chiral helical plasmonic nanostructure, made of gold and iron which can work as a mechanical sensor, allowing for the study of flow in complex fluid systems under circular dichroism spectroscopy. Under the influence of a rotating magnetic field, nanostructures are actuated resulting in a regulated optical response allowing for a nanorheological study. Synthesis of these nanohelices involved the use of block copolymer micelle nanolithography (BCML) [59]. The nanohelices formed from this are then coated in gold and iron using physical vapor GLAD. The ability of these nanohelices was demonstrated in their determination of the viscosity of a fluid with and without microparticles used to model cells and other components that influence the viscosity of fluids on the macroscale. Results displayed that there was no significant change in viscosities measured by the nanohelices. This is due to their nanosize and ability to distinguish the fluid from solid particles. When viscosities of the same two fluids were determined using the Krieger–Dougherty model, the viscosity of the fluid with microparticles was determined to be ten times that of the fluid without [125]. This design showed great potential in biomedical applications such as in the determination of blood plasma viscosity for diagnosis purposes. However, during experimentation, it was noted that protein coronas formed around the helices, affecting their dynamics. Further investigations can be carried out toward the use or development of materials that repel these proteins ensuring the preservation of nanohelix dynamics.

The flexible motion of magnetic micro/nanorobots also allows them to be effective biosensors for diagnosis. The propulsion of microrobots can accelerate the transport of analytes toward bioreceptors and achieve fast and sensitive sensing even for ultrasmall sample volume. After surface functionalization, micro/nanorobots have abilities to sense DNA, proteins, and cancer cells [126]. Recently, Molinero- Fernández et al. [127] developed a magnetic micromotor to rapidly detect C-reactive protein in preterm infants' plasma for neonatal sepsis diagnosis. The tubular micromotors comprise a graphene oxide outer layer for immobilizing antibody, an intermediate Ni magnetic layer, and a PtNPs catalytic inner layer. Although the movement of the micromotor is from the bubble propulsion of PtNPs catalytic layer fueled by H₂O₂, the magnetic layer is used to stop the flow operation, guide motion, and collect samples. Using a similar propulsion mechanism, Amouzadeh Tabrizi et al. [128] produced a MnO₂-PEI/Ni/Au nanomotor modified with aptamer KH₁C₁₂, which can specifically sense human promyelocytic leukemia cells (HL-60 cancer cells) in the human serum sample. MnO₂ can also generate oxygen bubbles using 1% H₂O₂ as a fuel. Ni nanoparticles in the nanomotor are used to magnetically guide its oxygen-propelled movement and isolate nanomotors. This nanomotor shows good sensitivity to HL-60 cancer cells and has a low limit of sensing of 250 cells/mL.

3.1.4. *In vitro* devices with advanced control systems

Motivated by a desire to gain a better understanding of mechanobiology for improved tissue engineering, Jing et al. [129] developed a micromachine with microforce sensing and regulating abilities. This enables the testing of forces on cells to understand the effects of them and the cell's physical limits allowing for the development of better-informed cell manipulation processes. The machines' integrated actuation and testing system also offer a less cluttered alternative to previous methods of investigating mechanobiology. The device is made up of compliant PDMS for sensing purposes, a silicone frame for mechanical strength and nickel body for magnetic actuation. The robot is capable of translational motion with speeds of 2 mm/s achieved under 10 mT. Under weaker magnetic fields, the robot exhibits rotational motion without locomotion. An advanced control system has been developed for this microrobot allowing for automated operation. When directing a microobject to a target, the control system tells the robot to either carry out a push or realign motion based on visual feedback to the control system and computations by the implemented algorithm. These two motions are applied as needed until the navigation task is completed allowing for robust, automated microobject direction. The control system also allows for regulation of the force applied in moving microobjects. A maximum force threshold is set before operation, and when this set threshold is reached the robot stops applying force to the microobject. This ability was tested at 6, 10, and 12 μ N with results showing that the robot applied about 2 μ N more than the threshold force. This was due to a lag between the sensor and the control system and the low resolution of the sensor (1.5 μ N). This system presents an integrated and automated method for mechanobiological research on cells allowing for investigations into how different magnitudes of force affect cell development at different stages. However, currently, the smallest size of microobject it can interact with is 10 μ m; therefore, it would need to be downsized to interact with smaller microobjects such as red blood cells. Size is also an issue for maneuvering in tight spaces as this requires the robot to constantly realign itself which makes such operations take longer. Finally, although the researchers have identified ways to overcome the current challenges faced with the control system, there is still room to improve responsivity and force resolution of the system.

Seeking to improve the abilities of microrobots in navigation, Li et al. [75] set up a smart rotating magnetic fields system which can adjust the direction of motion of Janus sphere microvehicles to allow for autonomous navigation in complex and dynamically changing biological environments. This is achieved by connecting the field generator with a charge-coupled device (CCD) camera which provides real-time visual feedback of microrobots and the unknown environment to an artificial

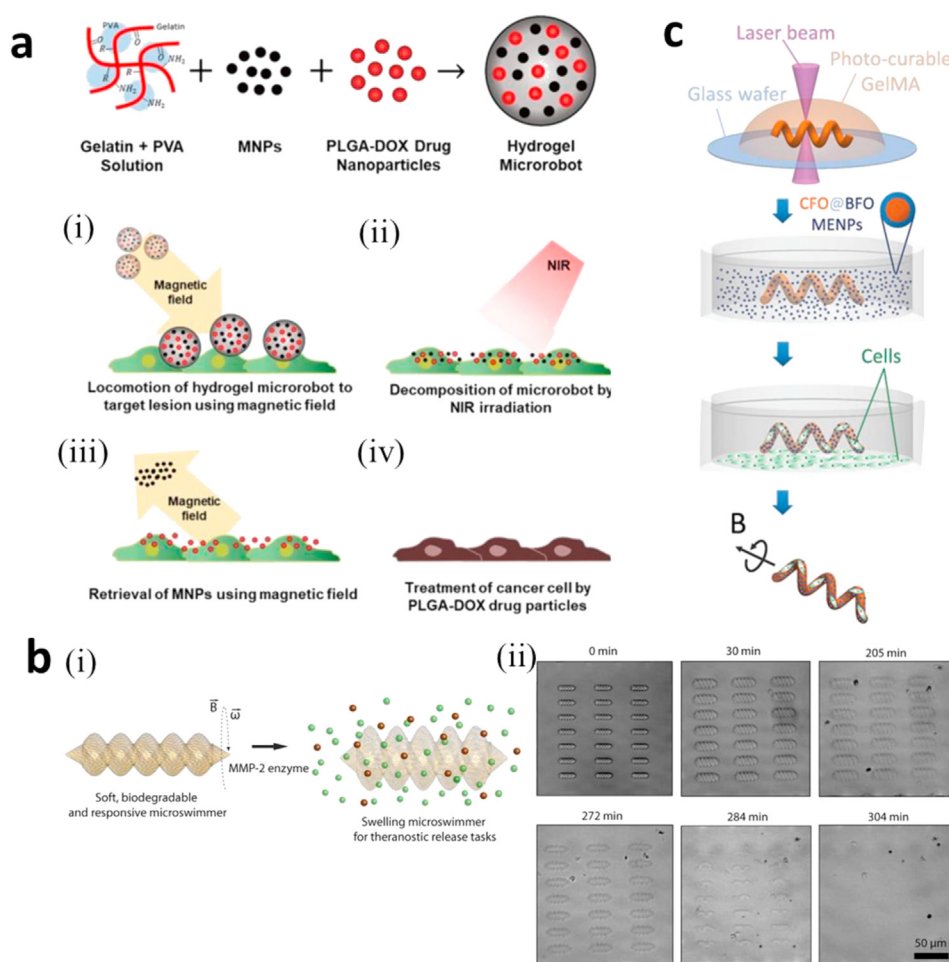
intelligence (AI) planner. The AI planner can intelligently construct a collision-free path for microrobots and give corresponding input signals to the magnetic field generator which then outputs programmable rotating fields to help microrobots to surmount obstacles. In the study, this system was also programmed to recognize cancer cells and guide microvesicles to them. A similar vision-back controlled system can be found in the recent study of Zarrouk et al. [130], where they added two microscopes to the vision section with a camera to observe magnetic microrobots in different scales.

3.2. *Biocompatibility and biodegradability of magnetic micro/nanorobots for clinical availability*

Although magnetic actuation is biocompatible depending on the strength of the magnetic field used, the biocompatibility and biodegradability of magnetically actuated micro/nanorobots themselves and the threat from the immune system (robots clearance before they execute tasks) are still limitations in their *in vivo* use.

To obtain magnetic actuation properties, robots always need to be coated or connected to magnetic materials, e.g. nickel, cobalt, and iron (e.g. NdFeB, Fe₃O₄ and FePt micro/nanoparticles). The biocompatibility of magnetic micro/nanoparticles is yet to be thoroughly assessed, but as has been mentioned in other studies nickel, for example, can be cytotoxic and its accumulation in the body could potentially lead to negative side effects [9,131]. To shield cytotoxic layers, titanium, as a known biocompatible material, has been used to cover them. In addition, as discussed in section 2.3, the incorporation of biological components, especially objects originating from human beings, in the design of robots can improve their biocompatibilities and reduce the cytotoxicity by eliminating biofouling effects. The recent rise of soft robots also serves a similar purpose. Despite the fact that many biocompatible micro/nanorobots have been developed and investigated to induce only minimal side effects in healthy tissue, there are still several refinements to be made before these are ready to be used in humans. One concern is the risk of the permanent retention of these devices in bodies. Current strategies for preventing retention include producing biodegradable robots and developing retrieval methods for non-biodegradable components. For example, several magnetic micro/nanorobots are made out of biodegradable materials such as PLGA, hydrogel, chitosan, and microalgae [78,132–135]. A microrobot proposed by Kim et al. [39] is biodegradable and allows for both controlled drug release and retrieval of potentially harmful MNPs after magnetic actuation is completed. The microrobot is made up of a gelatine/poly vinyl alcohol hydrogel containing MNPs and doxorubicin and is actuated by NIR radiation as well as magnetism (Fig. 12a). The microrobots can be navigated toward desired targets by magnetic actuation, and upon exposure to NIR radiation the hydrogels decompose releasing the MNPs and cancer drugs. A magnetic field is applied during the radiation step to prevent the uptake of MNPs. The released MNPs are brought together using a rotational magnetic field and subsequently retrieved using a rotating magnetic field gradient (Fig. 12a,i-iv). The robot's abilities were verified *in vitro* by its successful navigation through a Y-channel from an arbitrary start point to a target area followed by the aggregation and retrieval of MNPs. This is a big step forward in making magnetically actuated drug carriers safer for use *in vivo*; however, because of the large size of these microrobots (100–250 μ m), it is unable to operate in several blood vessels which limits its practical use. While the manufacture of similar, but smaller, robots is not necessarily an impossible task, the reduction in magnetic volume resulting from the smaller size would make magnetic actuation via field gradients more difficult so alternative means of actuation could be investigated for this purpose.

Hydrogels are a very promising material for biomedical applications because of their biodegradability and biocompatibility [132]. However, most hydrogel microrobots previously reported were propelled by means of magnetic field gradients, limiting their use in the human body because of the magnetic field strengths required to reach certain areas and



inability to properly navigate in flow systems. A helical hydrogel-based microrobot actuated by a rotating magnetic field by Lee et al. [137] proposes a new design for hydrogel robots that overcomes magnetic field gradient related challenges. Its hydrogel construction also enables NIR-stimulated drug release. The microrobot is fabricated by simply pumping the MNP containing hydrogel into an aqueous solution of calcium chloride using a syringe, causing chemical polymerization resulting in its spring-like shape. The resulting spring is then exposed to UV light for photopolymerization. The microrobot was heated in deionized water resulting in water loss, shrinkage, and creation of space for DOX to be loaded. The microrobot was actuated by a rotating magnetic field and was successfully navigated through a vascular phantom with speed increasing with field frequency until step out frequency of 2 Hz. When cultured with Hep3B cancer cells for 24 h, cell viabilities of 51.9% without stimulation and 19.5% with NIR stimulation were recorded. However, a significant challenge this design faces is its size (800 μm diameter) which limits its use. Research can be done into the development of a smaller version of this microrobot to be used as an intravenous drug carrier.

In regard to lowering the size of microrobots, recent studies discovered a photocurable, gelatin-methacryloyl (GelMA)-based hydrogel, which can be fabricated into much smaller biodegradable microrobots. Ceylan et al. [136] mixed GelMA with MNPs and used two-photon microprinting to produce a double helical magnetic hydrogel-based microrobot with length only of 20 μm . Importantly, the study further displayed the GelMA hydrogel contains specific cleavage sites for matrix metalloproteinase 2 (MMP-2) enzyme which is highly expressed in tumor ECM (Fig. 12b). Thus, this hydrogel microrobot can perform MMP-2 triggered degradation toward the tumor-targeted drug delivery

(controlled drug release) and specific diagnostic tasks. In addition, taking advantage of the GelMa hydrogel, Dong et al. [134] fabricated helical microrobots with 100 μm long via direct laser writing. After incorporating with magnetoelectric nanoparticles (CoFe₂O₄ core/BiFeO₃ shell), the microrobots can swim to the target lesion even with a low magnitude rotating magnetic field (a few millitesla). They can then be used as electrostimulators to activate the differentiation of neuronal cells under an alternating magnetic field (Fig. 12c). More importantly, the results showed that when these hydrogel microrobots fulfilled their therapeutic task, they can be completely degraded in 7 days by the enzymes in the ECM secreted by human neuroblastoma cells.

Although there are many strategies to lower the toxicity of magnetic micro/nanorobots to human bodies, the *in vivo* environment also poses dangers to micro/nanorobots. For example, as discussed earlier (section 2.3), the immune system is a critical obstacle for the *in vivo* application of micro/nanorobots. The microrobot will be recognized as an intruder by macrophages which then induce a series of immune responses to eliminate it. Despite the fact that biological objects (e.g. plasma cells' membrane coating) can provide help to micro/nanorobots in immune evasion, better understanding the interaction principles between the immune system and robots is essential for the safe design and clinical transformation of microrobots. Yasa et al. [138] recently proposed an opinion that for any medical small-scale robot design its immunogenicity is equally important with locomotion performance. In the study, they chose a magnetically driven helix and fully rigid microswimmer as the model and systematically investigated the influence of its surface morphology (same length, diameter, and volume but in three different turn numbers, 2, 5 and 10, respectively), size and surface chemistry (with or without PEG) on the immune response. The results showed that all these factors

have an impact on both locomotion and immunogenicity of microrobots but with complex entanglement. Specifically, they observed that the initial contact between the microrobots and the macrophage is through random physical encounter when macrophage probes the environment by using its filopodia. Then the macrophage will flatten over the microrobot surface to complete phagocytosis with favorable orientation. Thus, one confirmed principle about morphology-dependent phagocytosis is that an increase in the number of turns of a helical microrobot (i.e. higher surface area and surface area rate of change) is beneficial to slow down the phagocytosis process because macrophages need to use more energy to flatten over higher turn numbers. Consequently, the two-turns microrobot was the fastest to be engulfed even though it has the highest swimming speed. However, for the parameter of size, its impact on phagocytosis is indeterminate, which is cross-influenced by surface morphology of microrobots, such as the depth of helical grooves. The influence of surface chemistry on the immunogenicity of microrobots is the same as the results reported by many studies for nanomedicines [139, 140]. If the surface chemistry shows high resistivity to macromolecules corona formation, microrobots could gain more invisibility to macrophages. It should be noted that some sites of our body are immune-privileged, e.g. the eye and the central nervous system. Thus, when robots work in these areas, the locomotion performance can be the primary consideration in design.

3.3. Unique fabrication techniques to facilitate commercialization

This section covers novel fabrication techniques and the designs they have produced. A lot of these simplify the production of very similar already produced designs allowing for cheaper, quicker, and bulk manufacture of small-scale robots moving them toward commercial availability while others cover new techniques used to produce new designs to address challenges previously identified in other studies.

Work by Kim et al. [132] presented a new method of rapidly making drug carrying microrobots that allows for their mass production and simpler drug encapsulation as it does not require light exposure for polymerization. These microrobots were made up of PLGA, iron nanoparticles, and the drug to be carried. The fabrication process involved carving out desired shapes from polyvinyl alcohol sheets using laser micromachining to make templates for microrobots. These templates were then dipped into a solution of PLGA, MNPs, and the drug to be carried for about 5 s, then removed, and dried. The templates were removed by decomposing them in aqueous solution. This fabrication technique allows for easy tuning of robot characteristics such as MNP and drug concentration by simply altering their concentrations in solution and shape alteration for different purposes. The researchers also noted that they could potentially be used as building blocks for 3D assemblies. The drug release rate and speed in these robots can be controlled by varying iron content, with robots containing less iron moving faster under magnetic gradient and degrading slower, resulting in slower drug release. The robots were successfully manipulated by the EMA system and showed quick responses to directional changes. In addition, this method has the potential to be applied in the rotating magnetic fields with the fabrication of different shapes of robots. Cancer treatment abilities were demonstrated by culturing the microrobots with cancer cells for two days resulting in a cell survival rate of about 20%. The biodegradability and ease of manufacture of these microrobots are of great benefit to advancements in targeted drug therapy.

Cheang and Kim [141] proposed self-assembling microrobots and nanorobots made from MNPs. The self-assembly method of fabrication allows for cheaper, simpler, and quicker production of nanoswimmers and microswimmers than methods typically used such as electrodeposition, 3D printing, laser etching, and others. This fabrication first involved the dilution of 50–100 nm iron oxide magnetic particles in deionized water to a concentration of 0.1 mg/mL. The nanoparticles were then magnetized for a few seconds under a 5.06 mT magnetic field to produce single chains which served as the nanoswimmers as they retained a

nanoscale diameter. To produce the microswimmers, the single chains were further magnetized for a few minutes which caused them to aggregate into microswimmers of microscale diameter. Both structures are flexible and deform in motion because of hydrodynamics, and when actuated by a rotating magnetic field they form chiral shapes that produce propulsion during rotation. During testing, it was observed that the nanoswimmer moved in a jerky fashion because of Brownian motion. The effects of Brownian motion were much less severe in the microswimmer which produced much smoother movements, and moved at a speed of 3.6655 $\mu\text{m/s}$, than the nanoswimmer's 0.4912 $\mu\text{m/s}$ at the same magnetic field frequency of 10 Hz. This design could potentially be combined with drug-carrying nanoparticles and an efficient means of ensuring disassembly to produce nanorobots that release the drug bearing nanoparticles upon disassembly.

Alapan et al. [48] reported a fabrication mechanism that can flexibly produce specified and complex structures for microrobots. They took advantage of shape-encoded dielectrophoretic interactions to achieve dynamic self-assembly of mobile microrobots comprising diverse modules and reconfigurable locomotion modes. As illustrated in Fig. 13a, a series of microrobots consisting of magnetic 'microwheels' and 3D non-magnetic body were assembled and actuated by vertically and horizontally rotating magnetic fields. Because most materials are electrically polarizable, and the electric field gradient around each module can be precisely controlled by modifying its 3D shape; this fabrication technique enabled flexibility and programmability in design for robots performing complex tasks in medicine.

Ali et al. [142] proposed a hollow magnetic silica nanoswimmer fabricated using bacterial flagella as a biotemplate aimed at reducing costs of manufacture, enabling large-scale production of magnetic nanoswimmers. Because of the ability of bacterial flagella to morph into different conformations, these were used as templates to produce artificial flagella of different forms for different functions. The transcription of silica on the flagella was done by mixing a solution of the depolymerized flagella with an aqueous solution containing (3-aminopropyl)triethoxysilane and placing the mixture in an ice bath. Tetraethyl orthosilicate was then added to the mixture forming silica on the surface of the depolymerized flagella. Because of flagella's propensity to conform into the s-circular shape during standard templating conditions, researchers used their knowledge of pH-induced conformation change to maintain desired flagella geometry during templating. The nanotubes formed were coated with a nickel film approximately 10% of the thickness of the nanotubes by evaporation onto the dried tubes. The nanotubes were then magnetized and washed which depolymerizes flagella resulting in its release from nanotubes. The speed of these swimmers increased with frequency with no step-out behavior observed in the tested frequency range. From extrapolation of experimental results, it was found that at the frequency of rotation of bacterial flagella swimmers would swim at 22 $\mu\text{m/s}$, similar to actual bacteria's 25 $\mu\text{m/s}$. The fabrication technique presented in this work allows for mass production and for several geometric parameters to be adjusted by adjusting pH, initial concentrations, and nickel layer thickness. The use of silica also presents potential for biomedical applications due to factors such as their biocompatibility and porosity, allowing for high specific surface areas. Their specific surface areas open them up to use as excellent drug carriers because of increased capacity for bearing therapeutic agents.

Having noted issues with stem cell transplantation such as premature differentiation before reaching targets, low stem cell retention, and cell death and noting of these are all due to transportation in uncontrolled environments, Yasa et al. [21] presented a 3D printed microrobot which incorporates a recapitulated stem cell niche to overcome these issues. This robot consists of a double helical shell encapsulating a niche-like scaffolding, providing a controlled environment for the transportation of stem cells while also preconditioning them to differentiate into desired cell lineages (Fig. 13b). The microrobots were fabricated using a high-resolution 3D printer allowing for precise replication of cell niche conditions required by the stem cell, down to the micron level. The shell was

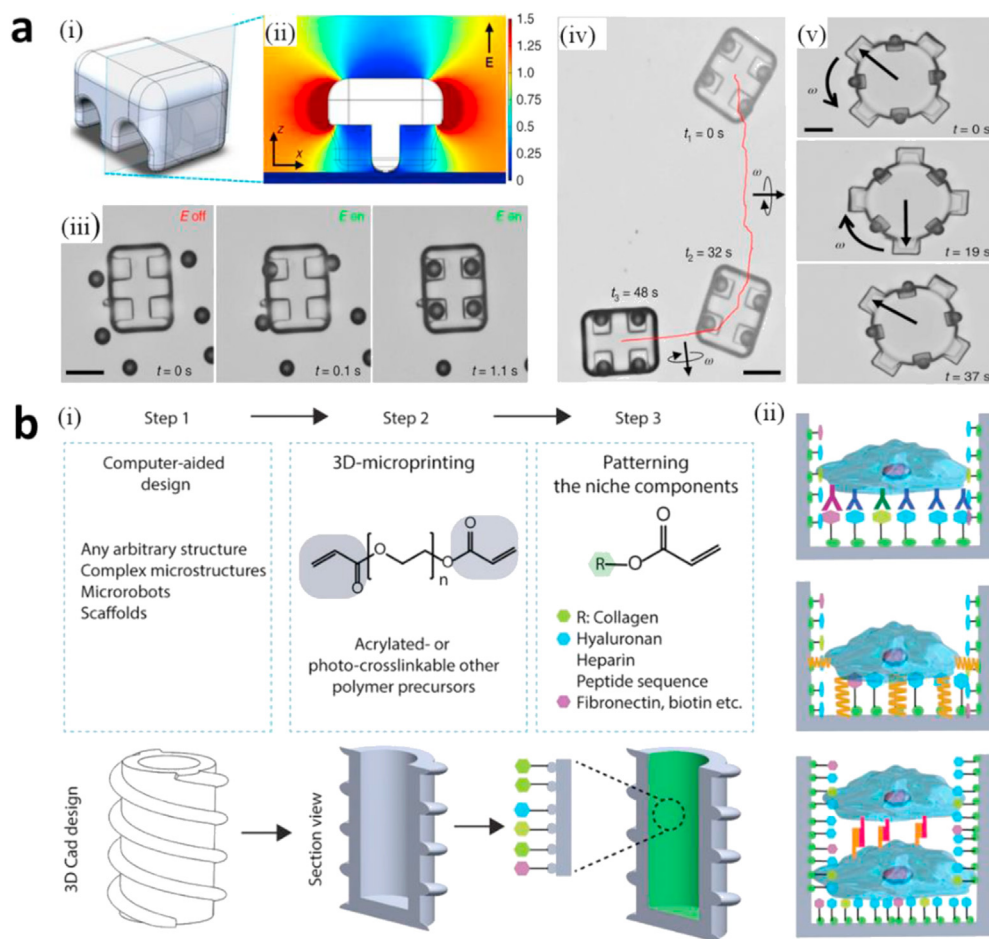


Fig. 13. (a) Shape-encoded assembly of magnetic microactuators to a non-magnetic body fabricated with direct laser writing. (i–ii) A 3D microcar body with four-wheel pockets is designed to generate site-selective attractive DEP forces toward the wheel pockets. Color bar: normalized electric field strength $(E/E_0)^2$. (iii) Directed assembly of the magnetic microactuators into the wheel pockets is realized on-demand using DEP. (iv) The microcar translates under a vertically rotating magnetic field and is steered by changing the rotation axis of the magnetic field. (v) The microrotor body and magnetic microbeads are coupled together with DEP and rotate when a horizontally rotating magnetic field in the x - y plane is applied. Scale bars, $25 \mu\text{m}$ [48]. (b) Patterning biological and physical aspects of a stem cell niche in a microbotic cell transporter (MCT). (i) The stepwise strategy of microbotic transporter fabrication and (ii) illustration of fine-tuned biochemical, biophysical, and cell-to-cell interactions between cells and their niche [21]. (All images are used with permission). DEP, dielectrophoretic.

made from a polymer, trimethylolpropane ethoxylate triacrylate (TMPETA), containing MNPs, and enabling propulsion via a corkscrew motion when exposed to a rotating magnetic field. TMPETA is known for its biocompatibility, and the use of cytotoxic metal coating for magnetic actuation was avoided by using MNPs incorporated into the polymer, further enhancing biocompatibility. The cell niche was made from gelatin, hyaluronan, and fibronectin and was constructed using a femtosecond laser. This fabrication method allows biological signals from the target tissue to be incorporated into the cell niche, enabling faster differentiation into target cell types. The resulting microbot performed better than its niche free counterparts in terms of cell retention and viability and swam at an average speed of $11.14 \pm 0.46 \mu\text{m/s}$. Despite addressing several issues identified in the use of stem cell transporters, this microbot is still limited by not being biodegradable and its inability to swim in non-Newtonian fluids which are found in several biological environments. Further studies can be done to address these issues and to gain an understanding of how these microtransporters and the stem cells inside them interact with tissue they may come in contact with during delivery to further advance these toward use *in vivo*.

4. Discussion: advantages, limitations, and challenges of micro/nanorobots

This paper aimed to investigate the current state of the art of magnetic nanorobots and microrobots in biomedicine suggests other biomedical applications for these devices and identify areas that would benefit from further research. This study revealed that the field of biomedical small-scale robots has experienced rapid advancements in the past few years, with successive incorporation of more complex technologies in their designs and a stronger focus on functionality and safety. It is also

indicated that the use of smart materials has greatly increased the functionality of these devices and allowed for on-demand execution of tasks.

This review of the literature enabled a comparison of the microrobots and nanorobots which clearly indicated areas or applications for which either is more capable or has significant advantages. For example, complex machinery and automation is certainly easier to implement in microrobots as they have the size advantage that allows for more components to be incorporated into a single device. That being said, nanorobots are quickly catching up in terms of complexity of designs and extra components being integrated into them. This suggests that this may soon no longer be a benefit of microrobots over nanorobots. The size of microrobots further proves useful in propulsion and direction, as Brownian motion has a far less significant effect on larger objects allowing for smooth operation and easy steering as opposed to jerky movements that may be observed in nanorobots. However, their size also poses limitations in their use *in vivo* as even some larger nanorobots risk being trapped in the smallest vasculature of animals that they are usually tested on [143]. The nanorobots size has allowed them to propel through complex viscoelastic media, far outperforming the microbot in all viscoelastic media despite producing negligible propulsion in water [72]. With the recently developed cell permeation and penetration methods, researchers are able to manipulate living cells with less risk of cell damage or death; researchers even envision one day operating nanorobots intracellularly [144]. All in all, although, in some cases, one scale of devices may have advantages over the other, they both occupy very important and usually different niches when it comes to biomedical applications; thus the field would benefit from continued research into both of them.

The biomedical applications of micro/nanorobots are mainly divided into *in vivo* and *in vitro* uses. Undoubtedly, drug targeting and

regenerative medicine fields stand to gain the most from these advancements with targeted triggered drug release and cell differentiation greatly enhancing the efficiency of such procedures. Small-scale robots are also becoming less hazardous for *in vivo* use with the development of biodegradable devices and the incorporation of MNPs into device structure rather than making devices from or coating with cytotoxic magnetic materials.

The various difficulties in the use of these devices generally and particularly *in vivo* persist despite many recent studies to identify ways of overcoming them. Relatedly, one of the major gaps in research identified in this study and which has received a lot of attention recently is the biocompatibility and biodegradability of the microrobot and nanorobot devices. The few empirical studies on this issue indicated that these devices have the potentials to harm body cells and tissues. The use of biodegradable materials, substances, and organisms along with MNPs in safe concentrations in the production of these devices is a big step toward tackling this issue. However, this solution poses another problem, which is that of MNPs accumulation in the body after biodegradation. Different means of retrieving MNPs and even whole devices are being considered in research. For example, Kim et al. [39] have attempted to use the rotational magnetic field gradient to aggregate and retrieve residual MNPs after degradation of hydrogel microrobot *in vitro*. The same group recently applied hydrogel microrobots for drug delivery to the eye followed by MNPs retrieval [145]. In addition, Iacovacci et al. [146] developed an intravascular magnetic catheter, allowing to collect up to 94% of the unused iron oxide nanoparticles from blood stream. However, this type of research is still at its infancy period, and there is undeniably a need for further studies that will attempt to determine what happens if said devices are used multiple times in one individual resulting in accumulation of MNP's beyond safe concentrations. Ran et al. [147] reported that if the concentration of Fe_3O_4 MNPs (~70 nm) beyond 25 $\mu\text{g}/\text{mL}$ *in vitro* and 12 mg/kg *in vivo* they will cause significant damage or apoptosis of erythrocytes. Recently, Malhotra et al. [148] published a review paper which summarized the studies in exploring the toxicity of various MNPs both *in vitro* and *in vivo*, but they found that when using different study models (from different publications) even similar MNPs can cause different toxicities. This is because besides properties of MNPs, the toxicity of MNPs may also depend on cell lines, organisms, immunogenicity, breakdown, and elimination from the body. More efforts and studies are needed in this field to build a reliable database for the safe usage of MNPs in clinical in the future.

Research that could investigate the development of coatings that will allow for drug loading and other biomedical multifunctionality could be conducted to evaluate the value of modifying the gold components on the likes of the free style and fish-like nanoswimmers. For example, they could be modified as with the protein-coated helical swimmers to allow for similar functionality such as pathogen diversion. In view of the potential for cytotoxicity of nickel which is commonly used in flexible swimmer designs, these devices could be further modified by reducing the amount of nickel in them or using researching less cytotoxic nickel alternatives.

Propulsion is probably the most matured aspect of research and development in the field of small-scale robots, with helical swimmers actuated with rotating magnetic fields being a standard for propulsion in low Re situations, as is the case for several biomedical applications. More recent research which examined oscillating magnetic fields and undulatory motion indicates that these features may be the future of propulsion for magnetically actuated robots because of their high speeds. Although it appears that despite this recognition, there have not been many proposed biomedical applications for them.

Another indication is that there is ongoing research to address the heterogeneity of fluid in biological systems and the difficulty of navigating them. With the numerous studies on the possibility of producing devices that change conformation in response to environmental stimuli such as temperature and pH and those that can propel themselves in complex viscoelastic environments, this field is on the way toward

overcoming this limitation. In terms of characterization, an important gap in research is how these devices will behave in flow conditions. This must be understood if these are to operate in the vascular network. The characterization of propulsion, however, is probably the most standardized of research fields in small-scale robot development, with many studies reporting velocities in terms of International System of Units' units as well as dimensionless units, for example, the body length per revolution unit. Perhaps other fields should also look into the development of dimensionless and standard characterization methods and parameters.

Micromachines have seen further development toward being able to carry out very ambitious functions despite the limitations they face in terms of remote powering and control. Some micromachines have advanced control schemes integrated into their control platforms to enable automation or complex remote control. Although their potential for use within the body is limited because of their dependence on visual feedback, their development greatly enhances the study of cell behavior *in vitro* and has enabled new means of cell manipulation. A review of the state of the art of small-scale robots carried out in 2017 indicated that at the time micromachines could only accomplish simple mechanical tasks. Examples of these tasks include gripping, drilling, and scraping [13]. However, recent design developments such as the ability for a microrobot to regulate the force it applies to cells are indications of more successful research in the attempt to design micromachines that will accomplish more complex tasks.

With some designs having been extensively studied in terms of effective propulsion and modifications that expand functionality, there has also been a rise in research toward the refinement of their fabrication processes with a focus on ensuring consistency, reproducibility, and large-scale production. These fabrication techniques demonstrate that commercialization may indeed be a valid prospect of these designs. Batch manufacture processes improve ease of scalability and allow for testing on multiple devices to improve reliability of experimental results. It also opens researchers up to research into the potential applications of multiple units of the same device, further expanding the research field. In contrast to the methods that allow for large-scale production, fabrication methods such as that used in the making of the artificial stem cell niche indicate that research is also going into the development of extremely precise methods of fabrication that enable the tuning of the finest details and reproduction of intricate biological systems.

However, for the clinical transformation of micro/nanorobots, there are many concerns proposed by previous reviews, for example, robot localization in body, communication, ease of fabrication, and undesired immunological reactions [8,10–12,149]. Biomedical micro/nanorobots have been expected to perform their work in every corner of the human body in clinic. Apart from precise control, precise real-time tracking of a single robot inside body could be the urgent challenge at the present especially for those operating in deep tissue areas. Pané et al. [150] detailed various imaging technologies which have been used to monitor biomedical micro/nanorobots *in vivo*, including MRI, X-ray imaging, ultrasound imaging, and fluorescence imaging. In those imaging methods, magnetic field and X-ray have large imaging depth (full body), and magnetic micro/nanorobots could provide intrinsic MRI during therapy if their magnetic components comprise MRI contrast agents, e.g. superparamagnetic nanoparticles [58]. However, these two imaging technologies are limited by spatiotemporal resolution, and the actuating and imaging magnetic fields for magnetic robots should be separated. In contrast, ultrasound and fluorescence can provide high spatial resolution and real-time imaging, but penetration depths are relatively low [151]. Thus, it is still a challenge currently to real-time track the position and state of these tiny robots in the deep tissue with microscale or nanoscale resolution. Future studies should consider the improvement of the imaging depth together with the high resolution, such as the development of multimodal imaging [152,153]. Recently, some studies reported that the cooperation of photoacoustic imaging

technology to micro/nanorobots can achieve high imaging resolution in relatively deep tissues (e.g. 2 cm in Wei's study [154]) and real-time tracking *in vivo* [60,154–156]. In addition, Iacovacci et al. [100] reported the successful tracking of a single magnetic microrobot with a diameter of 100 μm in *ex vivo* mouse abdomen via single-photon emission computed tomography (SPECT) imaging. Technetium-99m-based radioactive compounds were encapsulated in the microrobot structure as contrast agents. The study can clearly observe the shape change of the single microrobot, and the SPECT imaging is more efficient in distinguishing microrobots from the surrounding tissues.

A major finding of this study which corroborates the findings of Soto and Chrostowski [157] is that most research in this field focuses on tackling a single challenge which in itself may be a challenge facing the commercial or widespread use of magnetic small-scale robots. It will be essential to apply micro/nanorobots to practical and important applications and address systematic challenges – a key to demonstrate the value of the field. It should be recognized that the importance of such research will be sensitizing stakeholders such as pharmaceutical companies to the potential benefits of the end goals of this research. Client interest will generate funding and could potentially fast track the process of commercialization through their knowledge of regulation in the development of new therapies.

5. Conclusions and future perspectives

This review summarized recent advancements in small-scale robots used for biomedical applications, covering their design, and fabrication, described their *in vivo* and *in vitro* applications, and discussed considerations toward the clinical use of these micro/nanorobots. Micro/nanorobots have the potential to be used in deep tissue for real-time control and monitoring and for accomplishing complex tasks, but there are also many challenges including robot localization in body, communication, ease of fabrication, undesired immunological reactions, biocompatibility, biodegradability, difficulty in control of nanorobots in deep tissues, and design of nanorobots to perform complex tasks. While the field of small-scale robot research is relatively new and still in its highly innovative stages, more focused research must be continued to make these devices more functional and reliable. These research efforts must become concerted so that there will be some form of standardization of characterization techniques and parameters of various functions of the devices. However, it is recognized that in the more developed areas of study such as in propulsion a dimensionless speed or velocity measure has been introduced to allow for direct comparison between designs even if they are at different length scales. This may be an indication that as the study of other fields within biomedical small-scale robots matures standardized means of characterization may be introduced allowing researchers to properly weigh up the benefits of their designs over others. Concerted efforts also have further benefits; for example, they may lead to increased awareness of the potential of these devices which can generate client interest, thereby fast tracking commercialization. They could also lead to modifications of already existing designs to improve functionality, for example, the modification of the flexible swimmers with functional components for pathogen diversion as discussed in Section 4. In terms of fabrication techniques, both large-scale and precision-focused types of fabrication are immensely beneficial in small-scale robot development. There should be further research to evaluate how the fabrication of designs that have been successful *in vivo* can be developed into large-scale production techniques to move these devices further toward their eventual use in practical applications. For the use of micro/nanorobots in deep tissues, miniature devices may be established for local stimulation and imaging. Notwithstanding this, as this field continues to expand, both in terms of numbers of researchers and breadth of research, small-scale robots

continue to show their potential for use in biomedical applications. Studies of this nature can help to point out trends in research and identify areas that may benefit from collaborative research aimed at overcoming the current challenges of these devices, particularly in their use for clinical applications.

Declaration of competing interest

The authors declare that they have no known competing financial interests or personal relationships that could have appeared to influence the work reported in this paper.

Acknowledgement

This work was supported by the Royal Society of Edinburgh and National Natural Science Foundation of China (RSE-NFSC) International Joint Project Grant (60633) and the Cancer Research UK (CRUK) Grant for cancer early diagnosis.

References

- [1] Y. Yang, H. Wang, Perspectives of nanotechnology in minimally invasive therapy of breast cancer, *J. Healthc. Eng.* 4 (1) (2013) 67–86, <https://doi.org/10.1260/2040-2295.4.1.67>.
- [2] Z. Yaniv, C.A. Linte, When change happens: computer assistance and image guidance for minimally invasive therapy, *Healthc. Technol. Lett.* 1 (1) (2014) 2–5, <https://doi.org/10.1049/htl.2014.0058>.
- [3] B. Alekseev, E. Knyazev, M. Shkurnikov, D. Mikhailenko, A. Zotikov, K. Nyushko, A. Tonevitskiy, A. Kaprin, Mp28-10 panel of 6 microns for minimally invasive diagnosis of prostate cancer, *J. Urol.* 197 (4S) (2017) e341, <https://doi.org/10.1016/j.juro.2017.02.823>.
- [4] B.J. Nelson, I.K. Kaliaakatos, J.J. Abbott, Microrobots for minimally invasive medicine, *Annu. Rev. Biomed. Eng.* 12 (1) (2010) 55–85, <https://doi.org/10.1146/annurev-bioeng-010510-103409>.
- [5] J. Li, H. Wang, J. Cui, Q. Shi, Z. Zheng, T. Sun, Q. Huang, T. Fukuda, Magnetic micromachine using nickel nanoparticles for propelling and releasing in indirect assembly of cell-laden micromodules, *Micromachines* 10 (6) (2019) 370, <https://doi.org/10.3390/mi10060370>.
- [6] H.-H. Jeong, A.G. Mark, T.-C. Lee, M. Alarcón-Correa, S. Eslami, T. Qiu, J.G. Gibbs, P. Fischer, Active nanorheology with plasmonics, *Nano Lett.* 16 (8) (2016) 4887–4894, <https://doi.org/10.1021/acs.nanolett.6b01404>.
- [7] S. Martel, O. Felfoul, J.-B. Mathieu, A. Chanu, S. Tamaz, M. Mohammadi, M. Mankiewicz, N. Tabatabaei, MRI-based medical nanorobotic platform for the control of magnetic nanoparticles and flagellated bacteria for target interventions in human capillaries, *Int. J. Robot. Res.* 28 (9) (2009) 1169–1182, <https://doi.org/10.1177/0278364908104855>.
- [8] H. Ceylan, J. Giltinan, K. Kozielski, M. Sitti, Mobile microrobots for bioengineering applications, *Lab Chip* 17 (10) (2017) 1705–1724, <https://doi.org/10.1039/C7LC00064B>.
- [9] R. Fernandes, D.H. Gracias, Toward a miniaturized mechanical surgeon, *Mater. Today* 12 (10) (2009) 14–20, [https://doi.org/10.1016/S1369-7021\(09\)70272-X](https://doi.org/10.1016/S1369-7021(09)70272-X).
- [10] M. Sitti, H. Ceylan, W. Hu, J. Giltinan, M. Turan, S. Yim, E. Diller, Biomedical applications of untethered mobile milli/microrobots, *Proc. IEEE* 103 (2) (2015) 205–224, <https://doi.org/10.1109/JPROC.2014.2385105>.
- [11] J. Li, B. Esteban-Fernández de Ávila, W. Gao, L. Zhang, J. Wang, Micro/nanorobots for biomedicine: delivery, surgery, sensing, and detoxification, *Sci. Robot.* 2 (4) (2017), <https://doi.org/10.1126/scirobotics.aam6431> eaam6431.
- [12] M. Medina-Sánchez, H. Xu, O.G. Schmidt, Micro- and nano-motors: the new generation of drug carriers, *Ther. Deliv.* 9 (4) (2018) 303–316, <https://doi.org/10.4155/tde-2017-0113>.
- [13] X.-Z. Chen, M. Hoop, F. Mushtaq, E. Siringil, C. Hu, B.J. Nelson, S. Pané, Recent developments in magnetically driven micro- and nanorobots, *Appl. Mater. Today* 9 (2017) 37–48, <https://doi.org/10.1016/j.apmt.2017.04.006>.
- [14] Q.A. Pankhurst, J. Connolly, S.K. Jones, J. Dobson, Applications of magnetic nanoparticles in biomedicine, *J. Phys. D Appl. Phys.* 36 (13) (2003) R167–R181, <https://doi.org/10.1088/0022-3727/36/13/201>.
- [15] C. Alexiou, W. Arnold, R.J. Klein, F.G. Parak, P. Hulin, C. Bergemann, W. Erhardt, S. Wagenpfeil, A.S. Lübke, Locoregional cancer treatment with magnetic drug targeting, *Canc. Res.* 60 (23) (2000) 6641–6648, <http://www.ncbi.nlm.nih.gov/pubmed/11118047>.
- [16] V.S. Kalambur, B. Han, B.E. Hammer, T.W. Shield, J.C. Bischof, In vitro characterization of movement, heating and visualization of magnetic nanoparticles for biomedical applications, *Nanotechnology* 16 (8) (2005) 1221–1233, <https://doi.org/10.1088/0957-4484/16/8/041>.
- [17] R.S. Molday, D. Mackenzie, Immunospecific ferromagnetic iron-dextran reagents for the labeling and magnetic separation of cells, *J. Immunol. Methods* 52 (3) (1982) 353–367, [https://doi.org/10.1016/0022-1759\(82\)90007-2](https://doi.org/10.1016/0022-1759(82)90007-2).
- [18] A. Senyeyi, K. Widder, G. Czerlinski, Magnetic guidance of drug-carrying microspheres, *J. Appl. Phys.* 49 (6) (1978) 3578–3583, <https://doi.org/10.1063/1.325219>.

- [19] A.S. Lübbecke, C. Bergemann, W. Huhnt, T. Fricke, H. Riess, J.W. Brock, D. Huhn, Preclinical experiences with magnetic drug targeting: tolerance and efficacy, *Canc. Res.* 56 (20) (1996) 4694–4701, <https://cancerres.aacrjournals.org/content/56/20/4694>.
- [20] J. van der Zee, Heating the patient: a promising approach? *Ann. Oncol.* 13 (8) (2002) 1173–1184, <https://doi.org/10.1093/annonc/mdf280>.
- [21] I.C. Yasa, A.F. Tabak, O. Yasa, H. Ceylan, M. Sitti, 3D-Printed microbotic transporters with recapitulated stem cell niche for programmable and active cell delivery, *Adv. Funct. Mater.* 29 (17) (2019) 1808992, <https://doi.org/10.1002/adfm.201808992>.
- [22] S. Martel, Collective methods of propulsion and steering for untethered microscale nanorobots navigating in the human vascular network, *Proc. Inst. Mech. Eng. Part C J. Mech. Eng. Sci.* 224 (7) (2010) 1505–1513, <https://doi.org/10.1243/09544062JMES2079>.
- [23] A. Ghosh, P. Fischer, Controlled propulsion of artificial magnetic nanostructured propellers, *Nano Lett.* 9 (6) (2009) 2243–2245, <https://doi.org/10.1021/nl900186w>.
- [24] T. Honda, K.I. Arai, K. Ishiyama, Micro swimming mechanisms propelled by external magnetic fields, *IEEE Trans. Magn.* 32 (5) (1996) 5085–5087, <https://doi.org/10.1109/20.539498>.
- [25] V. Magdanz, I.S.M. Khalil, J. Simmchen, G.P. Furtado, S. Mohanty, J. Gebauer, H. Xu, A. Klingner, A. Aziz, M. Medina-Sánchez, O.G. Schmidt, S. Misra, IRONSperm: sperm-templated soft magnetic microrobots, *Sci. Adv.* 6 (28) (2020), <https://doi.org/10.1126/sciadv.aba5855> eaba5855.
- [26] T. Li, J. Li, H. Zhang, X. Chang, W. Song, Y. Hu, G. Shao, E. Sandraz, G. Zhang, L. Li, J. Wang, Magnetically propelled fish-like nanoswimmers, *Small* 12 (44) (2016) 6098–6105, <https://doi.org/10.1002/sml.201601846>.
- [27] T. Li, J. Li, K.I. Morozov, Z. Wu, T. Xu, I. Rozen, A.M. Leshansky, L. Li, J. Wang, Highly efficient freestyle magnetic nanoswimmer, *Nano Lett.* 17 (8) (2017) 5092–5098, <https://doi.org/10.1021/acs.nanolett.7b02383>.
- [28] T. Li, A. Zhang, G. Shao, M. Wei, B. Guo, G. Zhang, L. Li, W. Wang, Janus microdimer surface walkers propelled by oscillating magnetic fields, *Adv. Funct. Mater.* 28 (25) (2018) 1706066, <https://doi.org/10.1002/adfm.201706066>.
- [29] J. He, X. Qi, Y. Miao, H.-L. Wu, N. He, J.-J. Zhu, Application of smart nanostructures in medicine, *Nanomedicine* 5 (7) (2010) 1129–1138, <https://doi.org/10.2217/nmm.10.81>.
- [30] B.R. Donald, C.G. Levey, C.D. McGray, D. Rus, M. Sinclair, Untethered micro-actuators for autonomous micro-robot locomotion: design, fabrication, control, and performance, in: *Springer Tracts Adv. Robot.*, 2005, pp. 502–516, https://doi.org/10.1007/11008941_54.
- [31] D. Kim, Z. Hao, J. Ueda, A. Ansari, A 5 mg micro-bristle-bot fabricated by two-photon lithography, *J. Micromech. Microeng.* 29 (10) (2019) 105006, <https://doi.org/10.1088/1361-6439/ab309b>.
- [32] T. Hayakawa, S. Fukada, F. Arai, Fabrication of an on-chip nanorobot integrating functional nanomaterials for single-cell punctures, *IEEE Trans. Robot.* 30 (1) (2014) 59–67, <https://doi.org/10.1109/TRO.2013.2284402>.
- [33] J. Tang, L.W. Rogowski, X. Zhang, M.J. Kim, Flagellar nanorobot with kinetic behavior investigation and 3D motion, *Nanoscale* 12 (22) (2020) 12154–12164, <https://doi.org/10.1039/D0NR02496A>.
- [34] T. Nagamune, Biomolecular engineering for nanobio/bionanotechnology, *Nano Converg* 4 (1) (2017) 9, <https://doi.org/10.1186/s40580-017-0103-4>.
- [35] T.H. Woo, Feasibility study for radiation therapy using nano-robotics incorporated with three-dimensional (3D) printing, *Rend. Lincei.* 27 (4) (2016) 721–728, <https://doi.org/10.1007/s12210-016-0559-x>.
- [36] I.L. Sokolov, V.R. Cherkasov, A.A. Tregubov, S.R. Buiuciu, M.P. Nikitin, Smart materials on the way to theranostic nanorobots: molecular machines and nanomotors, advanced biosensors, and intelligent vehicles for drug delivery, *Biochim. Biophys. Acta Gen. Subj.* 1861 (6) (2017) 1530–1544, <https://doi.org/10.1016/j.bbagen.2017.01.027>.
- [37] R.D. Dsouza, K.P. Navin, T. Theodoridis, P. Sharma, Design, fabrication and testing of a 2 DOF compliant flexural microgripper, *Microsyst. Technol.* 24 (9) (2018) 3867–3883, <https://doi.org/10.1007/s00542-018-3861-y>.
- [38] J. Li, T. Li, T. Xu, M. Kiristi, W. Liu, Z. Wu, J. Wang, Magneto-acoustic hybrid nanomotor, *Nano Lett.* 15 (7) (2015) 4814–4821, <https://doi.org/10.1021/acs.nanolett.5b01945>.
- [39] D. in Kim, H. Lee, S. hyun Kwon, H. Choi, S. Park, Magnetic nano-particles retrievable biodegradable hydrogel microrobot, *Sensor. Actuator. B Chem.* 289 (15) (2019) 65–77, <https://doi.org/10.1016/j.snb.2019.03.030>.
- [40] J. Vyskočil, C.C. Mayorga-Martinez, E. Jablonská, F. Novotný, T. Ruml, M. Pumera, Cancer cells microsurgery via asymmetric bent surface Au/Ag/Ni microbotic scalpels through a transversal rotating magnetic field, *ACS Nano* 14 (7) (2020) 8247–8256, <https://doi.org/10.1021/acsnano.0c01705>.
- [41] T.W.R. Fountain, P.V. Kailat, J.J. Abbott, Wireless control of magnetic helical microrobots using a rotating-permanent-magnet manipulator, in: *2010 IEEE Int. Conf. Robot. Autom.*, IEEE, 2010, pp. 576–581, <https://doi.org/10.1109/ROBOT.2010.5509245>.
- [42] K. Kikuchi, A. Yamazaki, M. Sendoh, K. Ishiyama, K.I. Arai, Fabrication of a spiral type magnetic micromachine for trailing a wire, *IEEE Trans. Magn.* 41 (10) (2005) 4012–4014, <https://doi.org/10.1109/TMAG.2005.855155>.
- [43] W. Gao, X. Feng, A. Pei, C.R. Kane, R. Tam, C. Hennessy, J. Wang, Bioinspired helical microswimmers based on vascular plants, *Nano Lett.* 14 (1) (2014) 305–310, <https://doi.org/10.1021/nl404044d>.
- [44] A. Barbot, D. Decanini, G. Hwang, Wireless obstacle detection and characterization by multimodal helical nanoswimmers, in: *2015 IEEE Int. Conf. Robot. Autom.*, IEEE, 2015, pp. 3525–3530, <https://doi.org/10.1109/ICRA.2015.7139687>.
- [45] T.O. Tasci, P.S. Herson, K.B. Neeves, D.W.M. Marr, Surface-enabled propulsion and control of colloidal microwheels, *Nat. Commun.* 7 (1) (2016) 10225, <https://doi.org/10.1038/ncomms10225>.
- [46] D. Ahmed, T. Baasch, N. Blondel, N. Läubli, J. Dual, B.J. Nelson, Neutrophil-inspired propulsion in a combined acoustic and magnetic field, *Nat. Commun.* 8 (1) (2017) 1–8, <https://doi.org/10.1038/s41467-017-00845-5>.
- [47] C. Bi, M. Guix, B. Johnson, W. Jing, D. Cappelleri, Design of microscale magnetic tumbling robots for locomotion in multiple environments and complex terrains, *Micromachines* 9 (2) (2018) 68, <https://doi.org/10.3390/mi9020068>.
- [48] Y. Alapan, B. Yigit, O. Beker, A.F. Demirörs, M. Sitti, Shape-encoded dynamic assembly of mobile micromachines, *Nat. Mater.* 18 (11) (2019) 1244–1251, <https://doi.org/10.1038/s41563-019-0407-3>.
- [49] M. Liu, Y. Wang, Y. Kuai, J. Cong, Y. Xu, H.G. Piao, L. Pan, Y. Liu, Magnetically powered shape-transformable liquid metal micromotors, *Small* 15 (52) (2019) 1–7, <https://doi.org/10.1002/sml.201905446>.
- [50] M. Sun, X. Fan, X. Meng, J. Song, W. Chen, L. Sun, H. Xie, Magnetic biohybrid micromotors with high maneuverability for efficient drug loading and targeted drug delivery, *Nanoscale* 11 (39) (2019) 18382–18392, <https://doi.org/10.1039/C9NR06221A>.
- [51] S. Kim, S. Lee, J. Lee, B.J. Nelson, L. Zhang, H. Choi, Fabrication and manipulation of ciliary microrobots with non-reciprocal magnetic actuation, *Sci. Rep.* 6 (1) (2016) 30713, <https://doi.org/10.1038/srep30713>.
- [52] S. Schuerle, S. Erni, M. Flink, B.E. Kratochvil, B.J. Nelson, Three-Dimensional magnetic manipulation of micro- and nanostructures for applications in life sciences, *IEEE Trans. Magn.* 49 (1) (2013) 321–330, <https://doi.org/10.1109/TMAG.2012.2224693>.
- [53] O. Felfoul, A.T. Becker, G. Fagogenis, P.E. Dupont, Simultaneous steering and imaging of magnetic particles using MRI toward delivery of therapeutics, *Sci. Rep.* 6 (1) (2016) 33567, <https://doi.org/10.1038/srep33567>.
- [54] Y. Shi, N. Li, C. Tremblay, S. Martel, A piezoelectric robotic system for MRI targeting assessments of therapeutics during dipole field navigation, *IEEE/ASME Trans. Mechatronics* (2020), <https://doi.org/10.1109/TMECH.2020.3009829>.
- [55] J.J. Abbott, K.E. Peyer, M.C. Lagomarsino, L. Zhang, L. Dong, I.K. Kaliakatsos, B.J. Nelson, How should microrobots swim? *Int. J. Robot. Res.* 28 (11–12) (2009) 1434–1447, <https://doi.org/10.1177/0278364909341658>.
- [56] S. Klumpp, C.T. Lefèvre, M. Bennet, D. Favre, Swimming with magnets: from biological organisms to synthetic devices, *Phys. Rep.* 789 (2019) 1–54, <https://doi.org/10.1016/j.physrep.2018.10.007>.
- [57] Z. Yang, L. Zhang, Magnetic actuation systems for miniature robots: a review, *Adv. Intell. Syst.* 2 (9) (2020) 2000082, <https://doi.org/10.1002/aisy.202000082>.
- [58] J. Hwang, J. Kim, H. Choi, A review of magnetic actuation systems and magnetically actuated guidewire- and catheter-based microrobots for vascular interventions, *Intell. Serv. Robot.* 13 (1) (2020) 1–14, <https://doi.org/10.1007/s11370-020-00311-0>.
- [59] J. Han, J. Zhen, V. Du Nguyen, G. Go, Y. Choi, S.Y. Ko, J.O. Park, S. Park, Hybrid-actuating macrophage-based microrobots for active cancer therapy, *Sci. Rep.* 6 (2016) 28717, <https://doi.org/10.1038/srep28717>.
- [60] L. Xie, X. Pang, X. Yan, Q. Dai, H. Lin, J. Ye, Y. Cheng, Q. Zhao, X. Ma, X. Zhang, G. Liu, X. Chen, Photoacoustic imaging-trackable magnetic microswimmers for pathogenic bacterial infection treatment, *ACS Nano* 14 (3) (2020) 2880–2893, <https://doi.org/10.1021/acsnano.9b06731>.
- [61] S. Bianchi, V. Carmona Sosa, G. Vizsnyczai, R. Di Leonardo, Brownian fluctuations and hydrodynamics of a microhelix near a solid wall, *Sci. Rep.* 10 (1) (2020) 4609, <https://doi.org/10.1038/s41598-020-61451-y>.
- [62] A. Ghosh, D. Paria, G. Rangarajan, A. Ghosh, Velocity fluctuations in helical propulsion: how small can a propeller be, *J. Phys. Chem. Lett.* 5 (1) (2014) 62–68, <https://doi.org/10.1021/jz402186w>.
- [63] P. Fischer, A. Ghosh, Magnetically actuated propulsion at low Reynolds numbers: towards nanoscale control, *Nanoscale* 3 (2) (2011) 557–563, <https://doi.org/10.1039/C0NR00566E>.
- [64] M.M. Alcazare, M. Karttunen, T. Ala-Nissila, Propulsion and controlled steering of magnetic nanohelices, *Soft Matter* 15 (7) (2019) 1684–1691, <https://doi.org/10.1039/C8SM00037A>.
- [65] B. Jang, E. Gutman, N. Stucki, B.F. Seitz, P.D. Wendel-García, T. Newton, J. Pokki, O. Ergeneman, S. Pané, Y. Or, B.J. Nelson, Undulatory locomotion of magnetic multilink nanoswimmers, *Nano Lett.* 15 (7) (2015) 4829–4833, <https://doi.org/10.1021/acs.nanolett.5b01981>.
- [66] E.M. Purcell, Life at low Reynolds number, *Am. J. Phys.* 45 (1) (1977) 3–11, <https://doi.org/10.1119/1.10903>.
- [67] T. Mirkovic, M.L. Foo, A.C. Arsenault, S. Fournier-Bidoz, N.S. Zacharia, G.A. Ozin, Hinged nanorods made using a chemical approach to flexible nanostructures, *Nat. Nanotechnol.* 2 (9) (2007) 565–569, <https://doi.org/10.1038/nnano.2007.250>.
- [68] M. Sfakiotakis, D.M. Lane, J.B.C. Davies, Review of fish swimming modes for aquatic locomotion, *IEEE J. Ocean. Eng.* 24 (2) (1999) 237–252, <https://doi.org/10.1109/48.757275>.
- [69] I.S.M. Khalil, A.F. Tabak, Y. Hamed, M.E. Mitwally, M. Tawakol, A. Klingner, M. Sitti, Swimming back and forth using planar flagellar propulsion at low Reynolds numbers, *Adv. Sci.* 5 (2) (2018) 1700461, <https://doi.org/10.1002/advs.201700461>.
- [70] H. Xie, M. Sun, X. Fan, Z. Lin, W. Chen, L. Wang, L. Dong, Q. He, Reconfigurable magnetic microrobot swarm: multimode transformation, locomotion, and manipulation, *Sci. Robot.* 4 (28) (2019), eaav8006, <https://doi.org/10.1126/scirobotics.aav8006>.
- [71] W. Gao, D. Kagan, O.S. Pak, C. Clawson, S. Campuzano, E. Chuluun-Erdene, E. Shipton, E.E. Fullerton, L. Zhang, E. Lauga, J. Wang, Cargo-towing fuel-free

- magnetic nanoswimmers for targeted drug delivery, *Small* 8 (3) (2012) 460–467, <https://doi.org/10.1002/smll.201101909>.
- [72] D. Schamel, A.G. Mark, J.G. Gibbs, C. Miksch, K.I. Morozov, A.M. Leshansky, P. Fischer, Nanopropellers and their actuation in complex viscoelastic media, *ACS Nano* 8 (9) (2014) 8794–8801, <https://doi.org/10.1021/nn502360t>.
- [73] M.T. Taschuk, M.M. Hawkeye, M.J. Brett, Glancing angle deposition, in: *Handb. Depos. Technol. Film. Coatings*, Elsevier, 2010, pp. 621–678, <https://doi.org/10.1016/B978-0-8155-2031-3.00013-2>.
- [74] M. Pal, N. Somalwar, A. Singh, R. Bhat, S.M. Eswarappa, D.K. Saini, A. Ghosh, Maneuverability of magnetic nanomotors inside living cells, *Adv. Mater.* 30 (22) (2018) 1800429, <https://doi.org/10.1002/adma.201800429>.
- [75] T. Li, X. Chang, Z. Wu, J. Li, G. Shao, X. Deng, J. Qiu, B. Guo, G. Zhang, Q. He, L. Li, J. Wang, Autonomous collision-free navigation of microvehicles in complex and dynamically changing environments, *ACS Nano* 11 (9) (2017) 9268–9275, <https://doi.org/10.1021/acsnano.7b04525>.
- [76] S. Palagi, P. Fischer, Bioinspired microrobots, *Nat. Rev. Mater.* 3 (6) (2018) 113–124, <https://doi.org/10.1038/s41578-018-0016-9>.
- [77] J. Ali, U.K. Cheang, J.D. Martindale, M. Jabbarzadeh, H.C. Fu, M. Jun Kim, Bacteria-inspired nanorobots with flagellar polymorphic transformations and bundling, *Sci. Rep.* 7 (1) (2017) 14098, <https://doi.org/10.1038/s41598-017-14457-y>.
- [78] X. Yan, Q. Zhou, M. Vincent, Y. Deng, J. Yu, J. Xu, T. Xu, T. Tang, L. Bian, Y.-X.J. Wang, K. Kostarelos, L. Zhang, Multifunctional biohybrid magnetite microrobots for imaging-guided therapy, *Sci. Robot.* 2 (12) (2017) eaq1155, <https://doi.org/10.1126/scirobotics.aaq1155>.
- [79] S. Lauback, K.R. Mattioli, A.E. Marras, M. Armstrong, T.P. Rudibaugh, R. Sooryakumar, C.E. Castro, Real-time magnetic actuation of DNA nanodevices via modular integration with stiff micro-levers, *Nat. Commun.* 9 (1) (2018) 1446, <https://doi.org/10.1038/s41467-018-03601-5>.
- [80] S. Asakura, G. Eguchi, T. Iino, Reconstitution of bacterial flagella in vitro, *J. Mol. Biol.* 10 (1) (1964) 42–56, [https://doi.org/10.1016/S0022-2836\(64\)80026-7](https://doi.org/10.1016/S0022-2836(64)80026-7).
- [81] S. Asakura, T. Iino, Polymorphism of Salmonella flagella as investigated by means of in vitro copolymerization of flagellins derived from various strains, *J. Mol. Biol.* 64 (1) (1972) 251–268, [https://doi.org/10.1016/0022-2836\(72\)90334-8](https://doi.org/10.1016/0022-2836(72)90334-8).
- [82] X. Yan, J. Xu, Q. Zhou, D. Jin, C. Ian, Q. Feng, D.H.L. Ng, L. Bian, L. Zhang, Molecular cargo delivery using multicellular magnetic microswimmers, *Appl. Mater. Today*. 15 (2019) 242–251, <https://doi.org/10.1016/j.apmt.2019.02.006>.
- [83] V. Du Nguyen, V.H. Le, S. Zheng, J. Han, J.-O. Park, Preparation of tumor targeting cell-based microrobots carrying NIR light sensitive therapeutics manipulated by electromagnetic actuating system and Chemotaxis, *J. Micro-Bio Robot.* 14 (3–4) (2018) 69–77, <https://doi.org/10.1007/s12213-018-0110-5>.
- [84] M.S. Muthu, S.A. Kulkarni, A. Raju, S.-S. Feng, Theranostic liposomes of TPGS coating for targeted co-delivery of docetaxel and quantum dots, *Biomaterials* 33 (12) (2012) 3494–3501, <https://doi.org/10.1016/j.biomaterials.2012.01.036>.
- [85] S. Li, T. Tian, T. Zhang, X. Cai, Y. Lin, Advances in biological applications of self-assembled DNA tetrahedral nanostructures, *Mater. Today* 24 (2019) 57–68, <https://doi.org/10.1016/j.mat.2018.08.002>.
- [86] R. Dreyfus, J. Baudry, M.L. Roper, M. Fermigier, H.A. Stone, J. Bibette, Microscopic artificial swimmers, *Nature* 437 (7060) (2005) 862–865, <https://doi.org/10.1038/nature04090>.
- [87] H. Xu, M. Medina-Sánchez, V. Magdanz, L. Schwarz, F. Hebenstreit, O.G. Schmidt, Sperm-hybrid micromotor for targeted drug delivery, *ACS Nano* 12 (1) (2018) 327–337, <https://doi.org/10.1021/acsnano.7b06398>.
- [88] J. Li, P. Angsantikul, W. Liu, B. Esteban-Fernández de Ávila, X. Chang, E. Sandraz, Y. Liang, S. Zhu, Y. Zhang, C. Chen, W. Gao, L. Zhang, J. Wang, Biomimetic platelet-camoouflaged nanorobots for binding and isolation of biological threats, *Adv. Mater.* 30 (2) (2018) 1704800, <https://doi.org/10.1002/adma.201704800>.
- [89] C.-M.J. Hu, R.H. Fang, J. Copp, B.T. Luk, L. Zhang, A biomimetic nanosponge that absorbs pore-forming toxins, *Nat. Nanotechnol.* 8 (5) (2013) 336–340, <https://doi.org/10.1038/nnano.2013.54>.
- [90] M.R. Yeaman, Platelets in defense against bacterial pathogens, *Cell. Mol. Life Sci.* 67 (4) (2010) 525–544, <https://doi.org/10.1007/s00018-009-0210-4>.
- [91] J. Yu, B. Wang, X. Du, Q. Wang, L. Zhang, Ultra-extensible ribbon-like magnetic microswarm, *Nat. Commun.* 9 (1) (2018) 3260, <https://doi.org/10.1038/s41467-018-05749-6>.
- [92] H. Gu, Q. Boehler, H. Cui, E. Secchi, G. Savorana, C. De Marco, S. Gervasoni, Q. Peyron, T.-Y. Huang, S. Pane, A.M. Hirt, D. Ahmed, B.J. Nelson, Magnetic cilia carpets with programmable metachronal waves, *Nat. Commun.* 11 (1) (2020) 2637, <https://doi.org/10.1038/s41467-020-16458-4>.
- [93] M. Xie, W. Zhang, C. Fan, C. Wu, Q. Feng, J. Wu, Y. Li, R. Gao, Z. Li, Q. Wang, Y. Cheng, B. He, Bioinspired soft microrobots with precise magneto-collective control for microvascular thrombolysis, *Adv. Mater.* 32 (26) (2020) 2000366, <https://doi.org/10.1002/adma.202000366>.
- [94] M. Sitti, D.S. Wiersma, Pros and cons: magnetic versus optical microrobots, *Adv. Mater.* 32 (20) (2020) 1906766, <https://doi.org/10.1002/adma.201906766>.
- [95] I.S.M. Khalil, D. Mahdy, A. El Sharkawy, R.R. Moustafa, A.F. Tabak, M.E. Mitwally, S. Hesham, N. Hamdi, A. Klingner, A. Mohamed, M. Sitti, Mechanical rubbing of blood clots using helical robots under ultrasound guidance, *IEEE Robot. Autom. Lett.* 3 (2) (2018) 1112–1119, <https://doi.org/10.1109/LRA.2018.2792156>.
- [96] X.Z. Chen, J.H. Liu, M. Dong, L. Müller, G. Chatzipiripiridis, C. Hu, A. Terzopoulou, H. Torlakci, X. Wang, F. Mushtaq, J. Puigmartí-Luis, Q.D. Shen, B.J. Nelson, S. Pané, Magnetically driven piezoelectric soft microswimmers for neuron-like cell delivery and neuronal differentiation, *Mater. Horizons*. 6 (7) (2019) 1512–1516, <https://doi.org/10.1039/c9mh00279k>.
- [97] V. Ball, Polydopamine nanomaterials: recent advances in synthesis methods and applications, *Front. Bioeng. Biotechnol.* 6 (2018) 109, <https://doi.org/10.3389/fbioe.2018.00109>.
- [98] G. Mandriota, R. Di Corato, M. Benedetti, F. De Castro, F.P. Fanizzi, R. Rinaldi, Design and application of cisplatin-loaded magnetic nanoparticle clusters for smart chemotherapy, *ACS Appl. Mater. Interfaces* 11 (2) (2019) 1864–1875, <https://doi.org/10.1021/acsami.8b18717>.
- [99] F. Ding, X. Gao, X. Huang, H. Ge, M. Xie, J. Qian, J. Song, Y. Li, X. Zhu, C. Zhang, Polydopamine-coated nucleic acid nanogel for siRNA-mediated low-temperature photothermal therapy, *Biomaterials* 245 (2020) 119976, <https://doi.org/10.1016/j.biomaterials.2020.119976>.
- [100] V. Iacovacci, A. Blanc, H. Huang, L. Ricotti, R. Schibli, A. Mencias, M. Behe, S. Pané, B.J. Nelson, High-resolution SPECT imaging of stimuli-responsive soft microrobots, *Small* 15 (34) (2019) 1900709, <https://doi.org/10.1002/smll.201900709>.
- [101] G. Go, V. Du Nguyen, Z. Jin, J.-O. Park, S. Park, A thermo-electromagnetically actuated microrobot for the targeted transport of therapeutic agents, *Int. J. Contr. Autom. Syst.* 16 (3) (2018) 1341–1354, <https://doi.org/10.1007/s12555-017-0060-z>.
- [102] X.-Z. Chen, M. Hoop, N. Shamsudhin, T. Huang, B. Özkale, Q. Li, E. Siringil, F. Mushtaq, L. Di Tizio, B.J. Nelson, S. Pané, Hybrid magnetoelectric nanowires for nanorobotic applications: fabrication, magneto-electric coupling, and magnetically assisted in vitro targeted drug delivery, *Adv. Mater.* 29 (8) (2017) 1605458, <https://doi.org/10.1002/adma.201605458>.
- [103] F. Mushtaq, H. Torlakci, M. Hoop, B. Jang, F. Carlson, T. Grunow, N. Läubli, A. Ferreira, X. Chen, B.J. Nelson, S. Pané, Motile piezoelectric nanowires for targeted drug delivery, *Adv. Funct. Mater.* 29 (12) (2019) 1808135, <https://doi.org/10.1002/adfm.201808135>.
- [104] T. Ozel, G.R. Bourret, C.A. Mirkin, Coaxial lithography, *Nat. Nanotechnol.* 10 (4) (2015) 319–324, <https://doi.org/10.1038/nnano.2015.33>.
- [105] S. Betal, A.K. Saha, E. Ortega, M. Dutta, A. Kumar, A.S. Bhalla, R. Guo, Core-shell magnetoelectric nanorobot – a remotely controlled probe for targeted cell manipulation, *Sci. Rep.* 8 (2018) 1755, <https://doi.org/10.1038/s41598-018-20191-w>.
- [106] Z. Wu, Y. Wu, W. He, X. Lin, J. Sun, Q. He, Self-propelled polymer-based multilayer nanorockets for transportation and drug release, *Angew. Chem. Int. Ed.* 52 (27) (2013) 7000–7003, <https://doi.org/10.1002/anie.201301643>.
- [107] X. Wang, J. Cai, L. Sun, S. Zhang, D. Gong, X. Li, S. Yue, L. Feng, D. Zhang, Facile fabrication of magnetic microrobots based on spirulina templates for targeted delivery and synergistic chemo-photothermal therapy, *ACS Appl. Mater. Interfaces* 11 (5) (2019) 4745–4756, <https://doi.org/10.1021/acsami.8b15586>.
- [108] J. Hu, S. Huang, L. Zhu, W. Huang, Y. Zhao, K. Jin, Q. ZhuGe, Tissue plasminogen activator-porous magnetic microrods for targeted thrombolytic therapy after ischemic stroke, *ACS Appl. Mater. Interfaces* 10 (39) (2018) 32988–32997, <https://doi.org/10.1021/acsami.8b09423>.
- [109] S. Lee, S. Kim, S. Kim, J.-Y. Kim, C. Moon, B.J. Nelson, H. Choi, A capsule-type microrobot with pick-and-drop motion for targeted drug and cell delivery, *Adv. Healthc. Mater.* 7 (9) (2018) 1700985, <https://doi.org/10.1002/adhm.201700985>.
- [110] S. Lee, J. Kim, J. Kim, A.K. Hoshair, J. Park, S. Lee, J. Kim, S. Pané, B.J. Nelson, H. Choi, A needle-type microrobot for targeted drug delivery by affixing to a microtissue, *Adv. Healthc. Mater.* 9 (7) (2020) 1901697, <https://doi.org/10.1002/adhm.201901697>.
- [111] X. Feng, H. Dixon, H. Glen-Ravenhill, S. Karaosmanoglu, Q. Li, L. Yan, X. Chen, Smart nanotechnologies to target tumor with deep penetration depth for efficient cancer treatment and imaging, *Adv. Ther.* 2 (10) (2019) 1900093, <https://doi.org/10.1002/adtp.201900093>.
- [112] S. Schuerle, A.P. Soleimany, T. Yeh, G.M. Anand, M. Häberli, H.E. Fleming, N. Mirkhani, F. Qiu, S. Hauert, X. Wang, B.J. Nelson, S.N. Bhatia, Synthetic and living micropopplers for convection-enhanced nanoparticle transport, *Sci. Adv.* 5 (4) (2019), eaav4803, <https://doi.org/10.1126/sciadv.aav4803>.
- [113] Z. Wu, J. Troll, H.-H. Jeong, Q. Wei, M. Stang, F. Ziemssen, Z. Wang, M. Dong, S. Schnichels, T. Qiu, P. Fischer, A swarm of slippery micropopplers penetrates the vitreous body of the eye, *Sci. Adv.* 4 (11) (2018), eaat4388, <https://doi.org/10.1126/sciadv.aat4388>.
- [114] M. Muthana, A.J. Kennerly, R. Hughes, E. Fagnano, J. Richardson, M. Paul, C. Murdoch, F. Wright, C. Payne, M.F. Lythgoe, N. Farrow, J. Dobson, J. Conner, J.M. Wild, C. Lewis, Directing cell therapy to anatomic target sites in vivo with magnetic resonance targeting, *Nat. Commun.* 6 (1) (2015) 8009, <https://doi.org/10.1038/ncomms9009>.
- [115] J. Li, X. Li, T. Luo, R. Wang, C. Liu, S. Chen, D. Li, J. Yue, S. Cheng, D. Sun, Development of a magnetic microrobot for carrying and delivering targeted cells, *Sci. Robot.* 3 (19) (2018), eaat8829, <https://doi.org/10.1126/scirobotics.aat8829>.
- [116] J. Yu, D. Jin, K.F. Chan, Q. Wang, K. Yuan, L. Zhang, Active generation and magnetic actuation of microrobotic swarms in bio-fluids, *Nat. Commun.* 10 (1) (2019) 1–12, <https://doi.org/10.1038/s41467-019-13576-6>.
- [117] A. Aziz, M. Medina-Sánchez, N. Koukourakis, J. Wang, R. Kuschmierz, H. Radner, J.W. Czarnecki, O.G. Schmidt, Real-time IR tracking of single reflective micromotors through scattering tissues, *Adv. Funct. Mater.* 29 (51) (2019) 1905272, <https://doi.org/10.1002/adfm.201905272>.
- [118] D. Zhong, W. Li, Y. Qi, J. He, M. Zhou, Photosynthetic biohybrid nanoswimmers system to alleviate tumor hypoxia for FL/PA/MR imaging-guided enhanced radio-photodynamic synergetic therapy, *Adv. Funct. Mater.* 30 (17) (2020) 1910395, <https://doi.org/10.1002/adfm.201910395>.

- [119] E. Diller, M. Sitti, Three-Dimensional programmable assembly by untethered magnetic robotic micro-grippers, *Adv. Funct. Mater.* 24 (28) (2014) 4397–4404, <https://doi.org/10.1002/adfm.201400275>.
- [120] C. Pacchierotti, F. Ongaro, F. van den Brink, C. Yoon, D. Prattichizzo, D.H. Gracias, S. Misra, Steering and control of miniaturized untethered soft magnetic grippers with haptic assistance, *IEEE Trans. Autom. Sci. Eng.* 15 (1) (2018) 290–306, <https://doi.org/10.1109/TASE.2016.2635106>.
- [121] S.R. Goudy, I.C. Yasa, X. Hu, H. Ceylan, W. Hu, M. Sitti, Biodegradable untethered magnetic hydrogel milli-grippers, *Adv. Funct. Mater.* (2020) 2004975, <https://doi.org/10.1002/adfm.202004975>.
- [122] J.C. Breger, C. Yoon, R. Xiao, H.R. Kwag, M.O. Wang, J.P. Fisher, T.D. Nguyen, D.H. Gracias, Self-folding thermo-magnetically responsive soft microgrippers, *ACS Appl. Mater. Interfaces* 7 (5) (2015) 3398–3405, <https://doi.org/10.1021/am508621s>.
- [123] A. Barbot, H. Tan, M. Power, F. Seichepine, G.-Z. Yang, Floating magnetic microrobots for fiber functionalization, *Sci. Robot.* 4 (34) (2019), <https://doi.org/10.1126/scirobotics.aax8336> eaax8336.
- [124] S. Lee, S. Lee, S. Kim, C.-H. Yoon, H.-J. Park, J. Kim, H. Choi, Fabrication and characterization of a magnetic drilling actuator for navigation in a three-dimensional phantom vascular network, *Sci. Rep.* 8 (1) (2018) 3691, <https://doi.org/10.1038/s41598-018-22110-5>.
- [125] I.M. Krieger, T.J. Dougherty, A mechanism for non-Newtonian flow in suspensions of rigid spheres, *Trans. Soc. Rheol.* 3 (1) (1959) 137–152, <https://doi.org/10.1122/1.548848>.
- [126] L. Cai, H. Wang, Y. Yu, F. Bian, Y. Wang, K. Shi, F. Ye, Y. Zhao, Stomatocyte structural color-barcode micromotors for multiplex assays, *Natl. Sci. Rev.* 7 (3) (2020) 644–651, <https://doi.org/10.1093/nsr/nwz185>.
- [127] Á. Molinero-Fernández, L. Arruzza, M.Á. López, A. Escarpa, On-the-fly rapid immunoassay for neonatal sepsis diagnosis: C-reactive protein accurate determination using magnetic graphene-based micromotors, *Biosens. Bioelectron.* 158 (2020) 112156, <https://doi.org/10.1016/j.bios.2020.112156>.
- [128] M. Amouzadeh Tabrizi, M. Shamsipur, R. Saber, S. Sarkar, Isolation of HL-60 cancer cells from the human serum sample using MnO₂-PEI/Ni/Au/aptamer as a novel nanomotor and electrochemical determination of thereof by aptamer/gold nanoparticles-poly(3,4-ethylene dioxithiophene) modified GC electrode, *Biosens. Bioelectron.* 110 (2018) 141–146, <https://doi.org/10.1016/j.bios.2018.03.034>.
- [129] W. Jing, S. Chowdhury, D. Cappelleri, Magnetic mobile microrobots for mechanobiology and automated biomanipulation, in: *Microbiorobotics*, Elsevier, 2017, pp. 197–219, <https://doi.org/10.1016/B978-0-32-342993-1.00017-3>.
- [130] A. Zarrouk, K. Belharet, O. Tahri, Vision-based magnetic actuator positioning for wireless control of microrobots, *Robot. Autom. Syst.* 124 (2020) 103366, <https://doi.org/10.1016/j.robot.2019.103366>.
- [131] L.P. Felix, J.E. Perez, M.F. Contreras, T. Ravasi, J. Kosel, Cytotoxic effects of nickel nanowires in human fibroblasts, *Toxicol. Reports.* 3 (2016) 373–380, <https://doi.org/10.1016/j.toxrep.2016.03.004>.
- [132] J. young Kim, S. Jeon, J. Lee, S. Lee, J. Lee, B.O. Jeon, J.E. Jang, H. Choi, A simple and rapid fabrication method for biodegradable drug-encapsulating microrobots using laser micromachining, and characterization thereof, *Sensor. Actuator. B Chem.* 266 (2018) 276–287, <https://doi.org/10.1016/j.snb.2018.03.033>.
- [133] C. Peters, M. Hoop, S. Pané, B.J. Nelson, C. Hierold, Degradable magnetic composites for minimally invasive interventions: device fabrication, targeted drug delivery, and cytotoxicity tests, *Adv. Mater.* 28 (3) (2016) 533–538, <https://doi.org/10.1002/adma.201503112>.
- [134] M. Dong, X. Wang, X. Chen, F. Mushtaq, S. Deng, C. Zhu, H. Torlakcik, A. Terzopoulou, X. Qin, X. Xiao, J. Puigmartí-Luis, H. Choi, A.P. Pêgo, Q. Shen, B.J. Nelson, S. Pané, 3D-Printed soft magnetolectric microswimmers for delivery and differentiation of neuron-like cells, *Adv. Funct. Mater.* 30 (17) (2020) 1910323, <https://doi.org/10.1002/adfm.201910323>.
- [135] U. Bozuyuk, O. Yasa, I.C. Yasa, H. Ceylan, S. Kizilel, M. Sitti, Light-triggered drug release from 3D-printed magnetic chitosan microswimmers, *ACS Nano* 12 (9) (2018) 9617–9625, <https://doi.org/10.1021/acsnano.8b05997>.
- [136] H. Ceylan, I.C. Yasa, O. Yasa, A.F. Tabak, J. Giltinan, M. Sitti, 3D-Printed biodegradable microswimmer for theranostic cargo delivery and release, *ACS Nano* 13 (3) (2019) 3353–3362, <https://doi.org/10.1021/acsnano.8b09233>.
- [137] H. Lee, H. Choi, M. Lee, S. Park, Preliminary study on alginate/NIPAM hydrogel-based soft microrobot for controlled drug delivery using electromagnetic actuation and near-infrared stimulus, *Biomed. Microdevices* 20 (4) (2018) 103, <https://doi.org/10.1007/s10544-018-0344-y>.
- [138] I.C. Yasa, H. Ceylan, U. Bozuyuk, A. Wild, M. Sitti, Elucidating the interaction dynamics between microswimmer body and immune system for medical microrobots, *Sci. Robot.* 5 (43) (2020) eaaz3867, <https://doi.org/10.1126/scirobotics.aaz3867>.
- [139] Y. Zou, S. Ito, F. Yoshino, Y. Suzuki, L. Zhao, N. Komatsu, Polyglycerol grafting shields nanoparticles from protein corona formation to avoid macrophage uptake, *ACS Nano* 14 (6) (2020) 7216–7226, <https://doi.org/10.1021/acsnano.0c02289>.
- [140] R. Qiao, C. Fu, Y. Li, X. Qi, D. Ni, A. Nandakumar, G. Siddiqui, H. Wang, Z. Zhang, T. Wu, J. Zhong, S. Tang, S. Pan, C. Zhang, M.R. Whittaker, J.W. Engle, D.J. Creek, F. Caruso, P.C. Ke, W. Cai, A.K. Whittaker, T.P. Davis, Sulfoxide-containing polymer-coated nanoparticles demonstrate minimal protein fouling and improved blood circulation, *Adv. Sci.* 7 (13) (2020) 2000406, <https://doi.org/10.1002/advs.202000406>.
- [141] U.K. Cheang, M.J. Kim, Self-assembly of robotic micro- and nanoswimmers using magnetic nanoparticles, *J. Nanoparticle Res.* 17 (3) (2015) 145, <https://doi.org/10.1007/s11051-014-2737-z>.
- [142] J. Ali, U.K. Cheang, A. Darvish, H. Kim, M.J. Kim, Biotemplated flagellar nanoswimmers, *Apl. Mater.* 5 (11) (2017) 116106, <https://doi.org/10.1063/1.5001777>.
- [143] Z. Jin, K.T. Nguyen, G. Go, B. Kang, H.-K. Min, S.-J. Kim, Y. Kim, H. Li, C.-S. Kim, S. Lee, S. Park, K.-P. Kim, K.M. Huh, J. Song, J.-O. Park, E. Choi, Multifunctional nanorobot system for active therapeutic delivery and synergistic chemophotothermal therapy, *Nano Lett.* 19 (12) (2019) 8550–8564, <https://doi.org/10.1021/acs.nanolett.9b03051>.
- [144] Z. Zhou, Y. Piao, L. Hao, G. Wang, Z. Zhou, Y. Shen, Acidity-responsive shell-sheddable camptothecin-based nanofibers for carrier-free cancer drug delivery, *Nanoscale* 11 (34) (2019) 15907–15916, <https://doi.org/10.1039/C9NR03872H>.
- [145] D. Kim, H. Lee, S. Kwon, Y.J. Sung, W.K. Song, S. Park, Bilayer hydrogel sheet-type intraocular microrobot for drug delivery and magnetic nanoparticles retrieval, *Adv. Healthcare Mater.* 9 (13) (2020) 2000118, <https://doi.org/10.1002/adhm.202000118>.
- [146] V. Iacovacci, L. Ricotti, E. Sinibaldi, G. Signore, F. Vistoli, A. Menciasci, An intravascular magnetic catheter enables the retrieval of nanoagents from the bloodstream, *Adv. Sci.* 5 (9) (2018) 1800807, <https://doi.org/10.1002/advs.201800807>.
- [147] Q. Ran, Y. Xiang, Y. Liu, L. Xiang, F. Li, X. Deng, Y. Xiao, L. Chen, L. Chen, Z. Li, Eryptosis indices as a novel predictive parameter for biocompatibility of Fe₃O₄ magnetic nanoparticles on erythrocytes, *Sci. Rep.* 5 (1) (2015) 16209, <https://doi.org/10.1038/srep16209>.
- [148] N. Malhotra, J.-S. Lee, R.A.D. Liman, J.M.S. Ruallo, O.B. Villaflores, T.-R. Ger, C.-D. Hsiao, Potential toxicity of iron oxide magnetic nanoparticles: a review, *Molecules* 25 (14) (2020) 3159, <https://doi.org/10.3390/molecules25143159>.
- [149] H. Ceylan, I.C. Yasa, U. Kilic, W. Hu, M. Sitti, Translational prospects of untethered magnetic microrobots, *Prog. Biomed. Eng.* 1 (1) (2019), 012002, <https://doi.org/10.1088/2516-1091/ab22d5>.
- [150] S. Pané, J. Puigmartí-Luis, C. Bergeles, X. Chen, E. Pellicer, J. Sort, V. Počepcová, A. Ferreira, B.J. Nelson, Imaging technologies for biomedical micro- and nanoswimmers, *Adv. Mater. Technol.* 4 (4) (2019) 1800575, <https://doi.org/10.1002/admt.201800575>.
- [151] S.Y. Nam, L.M. Ricles, L.J. Suggs, S.Y. Emelianov, Imaging strategies for tissue engineering applications, *tissue eng. Part B Rev* 21 (1) (2015) 88–102, <https://doi.org/10.1089/ten.teb.2014.0180>.
- [152] A. Servant, F. Qiu, M. Mazza, K. Kostarelos, B.J. Nelson, Controlled, In vivo swimming of a swarm of bacteria-like microbotic flagella, *Adv. Mater.* 27 (19) (2015) 2981–2988, <https://doi.org/10.1002/adma.201404444>.
- [153] F. Yang, A. Skripka, M.S. Tabatabaei, S.H. Hong, F. Ren, A. Benayas, J.K. Oh, S. Martel, X. Liu, F. Vetrone, D. Ma, Multifunctional self-assembled supernanoparticles for deep-tissue bimodal imaging and amplified dual-mode heating treatment, *ACS Nano* 13 (1) (2019) 408–420, <https://doi.org/10.1021/acsnano.8b06563>.
- [154] T. Wei, J. Liu, D. Li, S. Chen, Y. Zhang, J. Li, L. Fan, Z. Guan, C. Lo, L. Wang, K. Man, D. Sun, Development of magnet-driven and image-guided degradable microrobots for the precise delivery of engineered stem cells for cancer therapy, *Small* 16 (41) (2020) 1906908, <https://doi.org/10.1002/sml.201906908>.
- [155] Z. Wu, L. Li, Y. Yang, P. Hu, Y. Li, S.-Y. Yang, L.V. Wang, W. Gao, A microbotic system guided by photoacoustic computed tomography for targeted navigation in intestines in vivo, *Sci. Robot.* 4 (32) (2019) eaax0613, <https://doi.org/10.1126/scirobotics.aax0613>.
- [156] Y. Yan, W. Jing, M. Mehrmohammadi, Photoacoustic imaging to track magnetic-manipulated micro-robots in deep tissue, *Sensors* 20 (10) (2020) 2816, <https://doi.org/10.3390/s20102816>.
- [157] F. Soto, R. Chrostowski, Frontiers of medical micro/nanorobotics: in vivo applications and commercialization perspectives toward clinical uses, *Front. Bioeng. Biotechnol.* 6 (2018) 170, <https://doi.org/10.3389/fbioe.2018.00170>.